

Dynamic Long-Term Modelling of Generation Capacity
Investment and Capacity Margins: a GB Market Case
Study

Dan Eager, Benjamin Hobbs and Janusz Bialek

April 2012

CWPE 1217 & EPRG 1201

Dynamic Long-Term Modelling of Generation Capacity Investment and Capacity Margins: a GB Market Case Study

EPRG Working Paper 1201

CWPE Working Paper 1217

Dan Eager, Benjamin Hobbs and Janusz Bialek

Abstract

Many governments who preside over liberalised energy markets are developing policies aimed at promoting investment in renewable generation whilst maintaining the level of security of supply customers have come to expect. Of particular interest is the mix and amount of generation investment over time in response to policies promoting high penetrations of variable output renewable power such as wind.

Modelling the dynamics of merchant generation investment in market environments can inform the debate. Such models need improved methods to calculate expected output, costs and revenue of thermal generation subject to varying load and random independent thermal outages in a power system with high penetrations of wind.

This paper presents a dynamic simulation model of the aggregated Great Britain (GB) generation investment market. The short-term energy market is simulated using probabilistic production costing based on the Mix of Normals distribution technique with a residual load calculation (load net of wind output). Price mark-ups due to market power are accounted for. These models are embedded in a dynamic model in which generation companies use a Value at Risk (VaR) criterion for investment decisions. An 'energy-only' market setting is used to estimate the economic profitability of investments and forecast the evolution of



security of supply. Simulated results for the GB market case study show a pattern of increased relative security of supply risk during the 2020s. In addition, fixed cost recovery for many new investments can only occur during years in which more frequent supply shortages push energy prices higher. A sensitivity analyses on a number of key model assumptions provides insight into factors affecting the simulated timing and level of generation investment. This is achieved by considering the relative change in simulated levels of security of supply risk metric such as de-rated capacity margins and expected energy unserved.

The model can be used as a decision support tool in policy design, in particular how to address the increased 'energy-only' market revenue risk facing thermal generation, particularly peaking units, that rely on a small number of high price periods to recover fixed costs and make adequate returns on investment.

Keywords Power generation economics, Mix of Normals distribution, Thermal power generation, Wind power generation.

JEL Classification O13, P4, Q4

Contact
Publication
Financial Support

d.eager@ed.ac.uk
January, 2012
UKERC NERC NE/C513169/1, Supergen Flexnet
program, U.S. NSF EFRI Grant 35879
www.eprg.group.cam.ac.uk

Dynamic Long-Term Modelling of Generation Capacity Investment and Capacity Margins: a GB Market Case Study

D. Eager, B. F. Hobbs, and J. W. Bialek

Abstract

Many governments who preside over liberalised energy markets are developing policies aimed at promoting investment in renewable generation whilst maintaining the level of security of supply customers have come to expect. Of particular interest is the mix and amount of generation investment over time in response to policies promoting high penetrations of variable output renewable power such as wind.

Modelling the dynamics of merchant generation investment in market environments can inform the debate. Such models need improved methods to calculate expected output, costs and revenue of thermal generation subject to varying load and random independent thermal outages in a power system with high penetrations of wind.

This paper presents a dynamic simulation model of the aggregated Great Britain (GB) generation investment market. The short-term energy market is simulated using probabilistic production costing based on the Mix of Normals distribution technique with a residual load calculation (load net of wind output). Price mark-ups due to market power are accounted for. These models are embedded in a dynamic model in which generation companies use a Value at Risk (VaR) criterion for investment decisions. An ‘energy-only’ market setting is used to estimate the economic profitability of investments and forecast the evolution of security of supply. Simulated results for the GB market case study show a pattern of increased relative security of supply risk during the 2020s. In addition, fixed cost recovery for many new

D. Eager is with the Institute for Energy Systems, The University of Edinburgh, EH9 3JL, UK, d.eager@ed.ac.uk

B. F. Hobbs is with the Department of Geography and Environmental Engineering, Johns Hopkins University, Baltimore, Maryland 21218, USA, bhobbs@jhu.edu.

J. W. Bialek is with the Energy Group, School of Engineering, The University of Durham, DH1 3LE, UK. Janusz.Bialek@durham.ac.uk

investments can only occur during years in which more frequent supply shortages push energy prices higher. A sensitivity analyses on a number of key model assumptions provides insight into factors affecting the simulated timing and level of generation investment. This is achieved by considering the relative change in simulated levels of security of supply risk metric such as de-rated capacity margins and expected energy unserved. These results provide insights into the increased ‘energy-only’ market revenue risk facing thermal generating units, particularly peaking units that rely on a small number of high price periods in order to recover fixed costs and make an adequate return on investment.

Index Terms

Power generation economics, Mix of Normals distribution, Thermal power generation, Wind power generation.

I. INTRODUCTION

When making an economic assessment of the potential for generating capacity investments, we must model varying loads (e.g., in the form of the load duration curve), the expected contribution of generating units to serving these loads, and the revenues they receive by doing so. It is helpful if the technique used is computationally fast, accurate and robust, especially when multi-year simulations of a market are to be repeatedly run. One approach is to use probabilistic production costing, a long established method for calculating the expected output and costs of a thermal generation system subject to varying load and random and independent forced outages [1, 2]. The first focus of this paper is the integration in a dynamic capacity investment simulation of a probabilistic production costing method that considers the annual load curve and convolves it with generator outages using the Mix of Normals distribution (MOND) approximation. This production costing method was first described in [3] and then extended and used for the calculation of equilibrium capacity investment in a power market in [4] and [5], respectively. In this study, the method is applied for the first time to a nonequilibrium setting as part of a dynamic market simulation.

The second focus of the work is to assess the impact of high penetrations of wind power on the investment risks associated with conventional thermal generation. Therefore the method above is extended to include a residual load calculation (load net of wind output) using empirical load and simulated wind data. This residual load data is then used in the MOND production costing model. Finally, the MOND model is incorporated in the dynamic investment model and

applied to a simplified GB power system for an assumed (exogenously increasing) installed wind capacity.

The goal of this research is to address concerns about whether ‘energy-only’ markets (i.e., without capacity mechanisms) with high penetrations of wind are capable of inducing timely generation investments over a long-term time frame. Examples of ‘energy-only’ markets currently operating include GB, Australia’s National Electricity Market, Alberta, Nordpool, Ontario and Midwest ISO. This is of particular interest to policy makers whose combined goals are to promote investment in renewable generation, maintain an adequate level of resources, and reduce customer costs.

The dynamic model employs classical control theory to capture the interactions between electricity supply and demand. It shares similarities with existing dynamic models of merchant generation investments (e.g., [6–9]), however this particular application to the GB market with a high wind penetration is unique. Furthermore, the production costing methods used by previous dynamic models are deterministic, and therefore underestimate average costs (due to Jensen’s inequality [10]).

This paper is organised as follows: in Section II, the dynamic investment model in which the MOND technique is embedded is described. Features of the investment decision element of the model are provided in Section III. In Section IV a MOND is formally defined and its application to a market situation is given. Section V describes input assumptions and the wind models used. The purpose of this paper is to present and illustrate a methodology. For the purposes of illustration, a number of assumptions are made that in an actual application would require careful validation. Results from the dynamic simulation of capacity investment in a system with an existing installed capacity similar to that of GB are given in Section VI and finally, Section VII presents conclusions.

II. THE INVESTMENT MARKET MODEL

Techniques from control theory are used to model market investment dynamics (Fig. 1). Because the model is dynamic, current market conditions (e.g., capacity under construction or retirements), prices and their predictions are fed back to the investment block, modifying the investment behaviour. The resulting investment decisions are then fed back to the pricing mechanism, hence closing the loop.

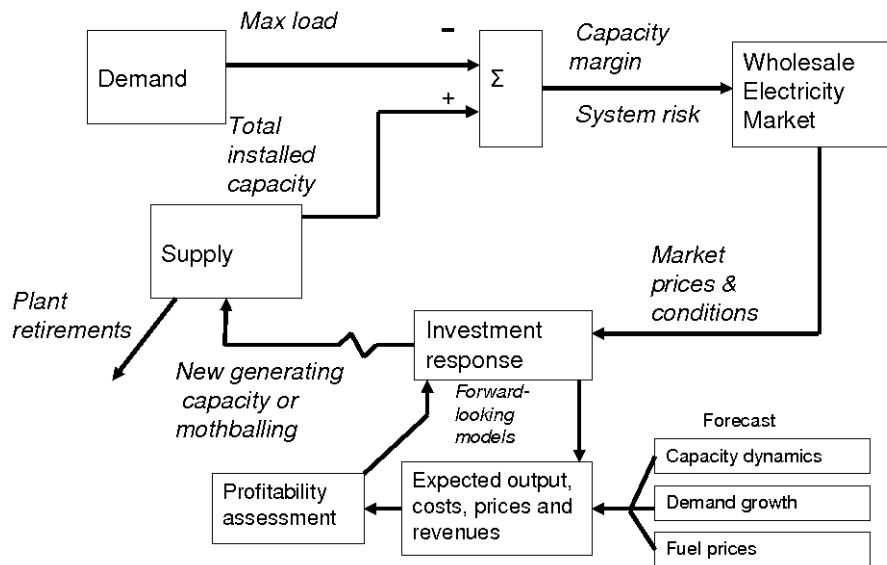


Fig. 1. Modelling generation capacity investment as a control problem; investment can be viewed as a negative feedback control mechanism with current and future energy prices (as a function of generation capacity margin) acting as a feedback signal.

The dynamics of the system concern the evolution of installed generation capacity and rate of demand growth. The rate of change in capacity at a particular time-step depends on new plant coming online or being de-mothballed net of any plant being retired or mothballed. Both are delayed signals from some earlier time. In the case of new plant, this delay is the lead time for construction, and in the case of retiring plant, this delay is the design lifetime. Mothballing requires zero delay, whilst de-mothballing requires a delay that is significantly less than full construction. An aggregate approach is taken whereby capacity is combined into five technology categories, namely nuclear, coal, wind, CCGT and OCGT, each with its own financial and technological characteristics.

The elegant notation used in [11] is employed to formally define the state of the system. That is, the state of the dynamic system is defined by the vectors (I_x, ψ_x) where $\psi_x = \{(\eta_j, \xi_j), i = 1 \dots n_x\}$ and $-\tau_x < \eta_1 < \eta_2 < \dots < \eta_{n_x}$. The ordering convention ensures that the oldest investment block ξ_1 will be completed first at time $\eta_1 + \tau_x$ [11]. Note that η_j indicates the time at which the decision is taken, and n_x is the number of projects of type x under construction. I_x is the installed capacity of plant type x , and τ_x is the expected build time. The index j provides the total number of non zero investment years since time zero. The control system is now defined

as the volume of installed capacity $I(t)$, which is a parallel cascade of the four technology categories. Each single category is defined by a Delay Differential Equation (DDE):

$$\frac{dI_x}{dt} = \sum_{(\eta_j, \xi_j) \in \psi_x} \xi_j \delta(t - \eta_j - \tau_x) - \sum_{(\eta_j, \xi_j) \in \psi_x} \xi_j \delta(t - \eta_j - \tau_x - \alpha_x), \quad (1)$$

where $\delta(t)$ is the Dirac delta function. The first term in (1) accounts for the addition of capacity ξ_j installed at time $\eta_j + \tau_x$. The second term accounts for deletion of capacity ξ_j built at time $\eta_j + \tau_x$ and retired at time $\eta_j + \tau_x + \alpha_x$, where α_x is the expected lifetime. The equation can be extended to include mothballing or premature retirement of capacity with an additional variable introduced to represent the lead time to de-mothball.¹ Each lump in (1) consists of a number of smaller components that represent individual generating units. These are 500 MW for nuclear and coal, 200 MW for CCGT and 50 MW for OCGT. Note that any mothballed capacity continues to age whilst it is “disconnected” from the system.

Evaluation of potential investments by generating firms is simulated by predicting future investment revenues and costs; this prediction uses market conditions in the “real-time” (actually, annual) energy market simulation as initial conditions and then predicts the future state of the system during the lifetime of a potential investment. Crucial uncertainties such as future demand, fuel prices and wholesale energy prices are all simulated in the prediction. The model does not consider the transmission network and is conceptually a single bus system.

III. GENERATION CAPACITY INVESTMENT

In order for adequate capacity to be maintained in the face of demand growth and retirement of existing capacity, investment in new capacity must be forthcoming. In this model the investment decision is taken annually and is considered an irreversible decision. It is based on the Net Present Value (NPV) of anticipated future profits.

A. Investment model logic

Investors are assumed to have the modelling capabilities available to formulate a reasonable approximation of the effect of wind generation on residual demand. That is, the investors are

¹Note that any mothballed capacity must continue to age whilst it is “disconnected” from the system to ensure it is permanently retired once it reaches the end of its design lifetime.

rational, but only within the limits of the information available to them, and thus do not possess perfect information about the future state of the system. This design follows the adaptive expectations hypothesis and has been applied in other dynamic models (e.g., [6, 8, 9, 12]). Plainly boom and bust type dynamics will be less severe if investors have rational expectations (see [13]) because they eliminate systematic forecast errors, however this is arguably not possible in most electricity markets owing to their relative infancy and ongoing modification [14]. These overshoot dynamics are further confounded by the limited forecasting certainty which modelling tools can provide concerning variables such as economic growth and future weather patterns. Note that variations in weather patterns are likely to average out to zero over the economic lifetime of an investment and thus do not affect decisions about capacity expansion.²

For simplicity, a single investor who is well acquainted with the structure of the market and capable of securing the necessary debt to finance large-scale plant investment is modelled. This representative agent approach has been used by other dynamic capacity market models (e.g., [14]). When estimating the profitability of an investment, a Monte Carlo (MC) approach is taken to obtain a probability distribution of profitability whereby estimates for conventional plant already under construction (including delays), demand growth, and fuel prices are considered stochastic.

The representative agent is aware of conventional plant already under construction at the start of each decision process. However there is uncertainty about a) the time remaining to build these plants, b) whether they will in fact make it to operation, and c) if rivals will jump in and invest in response to increases in expected profits. In the base case, generators assume all plant will come online with 100% certainty, and remaining build time is stochastic. This is modelled as the sum of the expected build time (minus one year) plus a random variable (r.v) that is sampled from a lognormal distribution, $lnN(\mu, \sigma^2)$, where μ and σ are the mean (one year) and standard deviation (six months) of the distribution, respectively. Decision making under uncertainty is modelled by taking a risk averse attitude to investment; this is discussed in the next sub-section. Currently operational plant is expected to generate for the duration of its design lifetime.

Fuel and carbon forward prices are based upon the UK Department of Energy and Climate Change (DECC) central case estimates [15, 16]. Assuming investor price forecasts are similar to

²Under the heroic assumption that climate change does not impact on future weather.

these estimates,³ the investor model uses the DECC estimate plus a r.v. to estimate future fuel prices. This r.v. is modelled as a mean reverting stochastic process with seasonality [18]:

$$dF_t = \alpha(m(t) - F_t)dt + v(F_t)dW_t, \quad (2)$$

$$m(t) = \frac{1}{\alpha} \frac{dq}{dt} + q(t), \quad (3)$$

where F_t is the price at time t , $q(t)$ is the DECC estimate, $m(t)$ is the time dependent mean reverting level which depends on the DECC estimate, v is the volatility, α is the speed of mean reversion and W is a standard one-dimensional Brownian motion [19]. Initially, $\alpha = 0.7$ in all cases (indicating a reasonably short excursion length) and v is 5%, 7%, 10% and 20% for uranium, coal, gas and carbon prices, respectively to reflect the relative price volatilities.

Investors consider annual load growth to be stochastic and is sampled from a Normal distribution. Our application assumes a mean of 0% and standard deviation of 1%. This is based on variations in demand growth [14] as well as the perception that economic growth could be offset by increased energy efficiency (e.g., [20]), thus allowing for small or even negative load growth.

The present value of an investment in technology x (i.e., nuclear, coal, CCGT, OCGT) at time τ_x is given by:

$$V_x = \sum_{i=\tau_x}^{\alpha_x} \frac{GM_x^i - FC_x}{(1+r)^{i-\tau_x}} - (IC_x + DC_x) \quad (4)$$

where $r = (\chi_x) \cdot \gamma + (1 - \chi_x) \cdot \epsilon_x$ is the firm's weighted average cost of capital (WACC), with χ_x and γ as the gearing ratio and expected bond return (assumed to be 8%) respectively, and ϵ_x is the required investor equity return. GM_x^i is the gross margin (cf. (24) or (37) depending on market bidding assumptions) for year i , FC_x is the generator fixed operating costs, and τ_x and α_x (cf. (1)) are both expressed in years. IC_x is the present worth of the investment cost:

$$IC_x = \sum_{i=0}^{\tau_x-1} M_i^x c_x p_x (1+r)^{-(i-\tau_x)}, \quad (5)$$

where p_x is the construction cost (£/MW), c_x is the plant capacity, M_i^x is the capital expenditure vector for the project with $\sum_{i=0}^{\tau_x-1} M_i^x = 1$. For simplicity, the expenditure schedule uses a lagged

³Which in the case of natural gas match quite well with available future prices from ICE Futures Europe (out to 2017) but are arguably a little low for coal - at the time of writing, Newcastle futures were rising at about 1.5% annually not falling by 6% as suggested by DECC [17].

formulation with

$$M_i^x = zM_{i+1}^x \quad (6)$$

where $z = 0.8$ (i.e., the capital outlay increases by 25% each year). Total interest accumulated during construction is given by $TIAC_x = IC_x - c_x p_x$. Finally, DC_x is the present worth of the decommissioning cost. Only nuclear projects have considerable decommissioning costs (estimated at 12% of p_x^4); in the case of other plant types the decommissioning liabilities are assumed to be offset by the salvage value of the assets [22]. Nuclear decommissioning is assumed to take 150 years and the equivalent incidence of capital outlay matrix contains 0.05 for the first 10 entries and (i.e., 50% of total decommissioning coming in first 10 years after closure) and the remaining entries are $1/140$ (i.e., 50% of cost spread over 140 years).

All cashflows are discounted to the start of the first year of operation. The total annualised costs per unforced MW (TAFC) (£/unfor.MW/yr) are given by:

$$TAFC_x = \frac{A_x^{crf}(IC_x + DC_x) + FC_x}{1 - \rho_x}, \quad (7)$$

where A_x^{crf} is the deferred capital recovery factor and ρ_x is the generator FOR.

Only the first n years of expected revenues are stochastically simulated by the investor (here $n = 7$); for the remaining years the (discounted) average of the simulated revenues are used (e.g., similar to [14]), i.e., assume that simulated prices for the first 7 years of plant operation are representative of the total expected plant lifetime. Furthermore, investors cap the total expected annual revenues received from scarcity rents (see Section IV-C) at the annualised cost of an OCGT. These actions ensure that expectations about future revenues are not unduly influenced by high forward simulated wholesale prices owing to generation retirements far in the future. No regulatory price caps are implemented in the real-time simulation.

Investors in peaking capacity (i.e., OCGT) assume an additional revenue of £10,000/unforced MW/yr can be obtained from the ancillary services (AS) market. AS revenues form a critical component of peaking capacity profitability, however they are insufficient by themselves to trigger investment and a combination of energy market and AS revenue is required in order to obtain adequate gross margins. Investors will not include AS revenues in the profitability calculation if OCGT capacity exceeds 8 GW (i.e., volume of installed OCGT capacity at the start of the

⁴Estimated to be between 9-12% by the World Nuclear Association [21].

simulation, c.f. Table III), this essentially limits the total obtainable revenue from AS if the volume of peaking capacity becomes large. However, in account of the point made above, this limit should not unduly dampen peaking capacity investment.

Because the model randomly samples capacity construction times, fuel prices and load growth, a large sample is required in order for investors to obtain reliable estimate of expected project value (4). Here, 100 MC simulation runs are carried out for each plant type in each decision year.

B. VaR criterion

Value at Risk (VaR) is a common criterion used in finance when investors place a high priority on avoiding poor outcomes (i.e., they are risk averse) [23]. Generally speaking, given a project value V , and defining the level of risk aversion by q , the VaR is defined as the value v_q such that $p(V \leq v_q) = 1 - q$.

In this model, the distribution of potential profits are constructed from the MC simulations of the stochastic variables and a risk averse investor with $q = 5\%$ is assumed. The distribution of V_x in (4) is computed by MC simulation for each plant type and an investment is deemed attractive if $p(V_x > V_x^{opt}) \geq (100 - q)\%$, where V_x^{opt} is the minimal acceptable V_x ; i.e., V_x^{opt} is a lower bound for the project value used in the VaR criterion. This is assumed to be zero (i.e., investors recover initial investment and receive adequate return on investment in account of the WACC applied in (4)).

The decision to mothball (or de-mothball), is based on the predicted gross margins over fixed operational costs (AGM) (£/MW) for the next three years of operation averaged over the MC simulation runs, i.e.,

$$AGM_x = \frac{1}{100} \sum_{j=1}^{100} \sum_{\forall j, i=1}^3 \frac{GM_x^i - FC_x}{(1+r)^i}. \quad (8)$$

If this is negative (or positive) then some currently operational (or offline) plant will be mothballed (or de-mothballed).

C. Modelling aggregate investment response

In some circumstances the expected profitability of new investments is extremely high, thus triggering a wave of new builds. In such cases, the investment rate will be limited by: 1) the

firm's beliefs about how many other market participants will move to invest; 2) the impact of new investment on the profitability of their existing plant; and 3) the ability of the firm to secure the debt required to fund multiple projects [8]. Using an aggregate investor response curve is useful in models of this type. For instance, in [14], the aggregate investment rate is increasing with the “*risk-adjusted forecast profit*”, which is derived from the investor's (risk averse, concave) utility function. Also in [8], an S-shaped nonlinear function of Profitability Index (PI) is used and various profitability functions are used in [7] to model investment rates based on managerial optimism concerning economic (i.e., expected profitability) and strategic (i.e., retaining market share) considerations.

In this paper, a function is applied to the outcome of the VaR decision rule in order to estimate the aggregate investment response of the market. This function is increasing with the expected profitability and is given by:

$$\xi_i = \max \left\{ 0, \xi_{max} \cdot \left(1 - e^{(-\beta \cdot PI_x^q)} \right) \right\}, \quad (9)$$

where

$$PI_x^q = \frac{V_x^q}{(IC_x + DC_x)} \quad (10)$$

is the Profitability Index (PI) (i.e., critical ($q\%$) V_x divided by investment cost per unit of capacity) and ξ_{max} is the maximum investment per year in technology x . ξ_{max} and β are calibrated so zero investment is made if $PI_x^q < PI_x^{opt}$ (with PI_x^{opt} the result of substituting V_x^{opt} into (10)), and $\xi_i = i_x$ volume of investment is made if $PI_x^q = 1$, where i_x is a fixed constant. Note that ξ_i provides the link to the state equation (1).

The function used in the base case is shown in Fig. 2 with fixed $i_x = 2$ GW and $\xi_{max} = 4$ GW, and $\beta = 0.7$ resulting from the calibration. Changing β alters the aggregate response, as shown by the dotted lines. There is the potential to include different response curves within each fuel or peak/base generator type (e.g., as in [8]). There is also an additional step whereby after each 2 GW of capacity of investment is triggered, the investor decision is re-run to ensure that no other plant types become more attractive in relation to other options as a result of this addition. This maintains the iterative adding characteristic in [24] whereby the decision is to 1) invest in the most profitable technology (if any), followed by 2) a re-run of the investment decision with all new investments accounted for. 1-2 are then repeated until no additional plants are profitable.

For multiple investments with $PI_x > 0$, the option with the highest PI_x is chosen. Finally, total annual investments are limited to 10% of installed capacity.

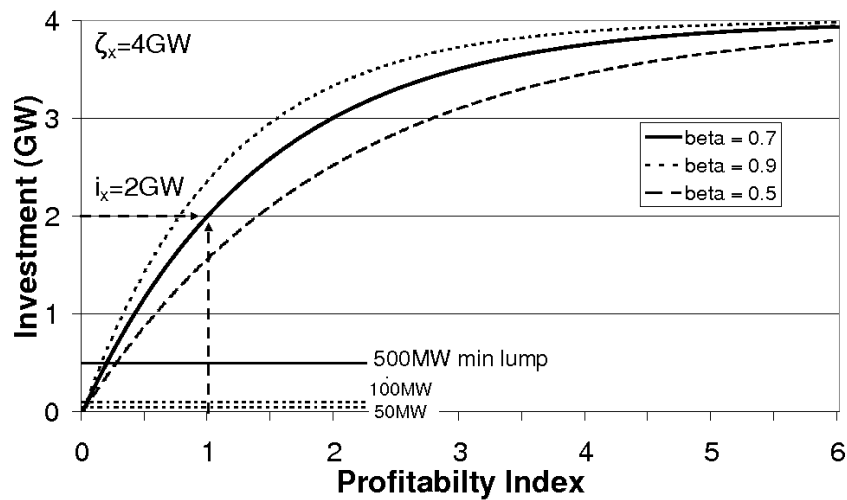


Fig. 2. Plot of model aggregate investment response curve defined by (9) (solid line) where $i_x = 2 \text{ GW}$ and $\xi_{max} = 4 \text{ GW}$. Also shown are the minimum investment lump sizes along with curves for different values of β .

The volume (GW) of plant mothballed or de-mothballed is determined simplistically using the linear function $\xi_i = \min(M, AGM_x/10^4)$, i.e., decreasing or increasing in AGM_x (£/MW) up to a maximum of M GW (Fig. 3). In this case M is chosen to be 2 GW.

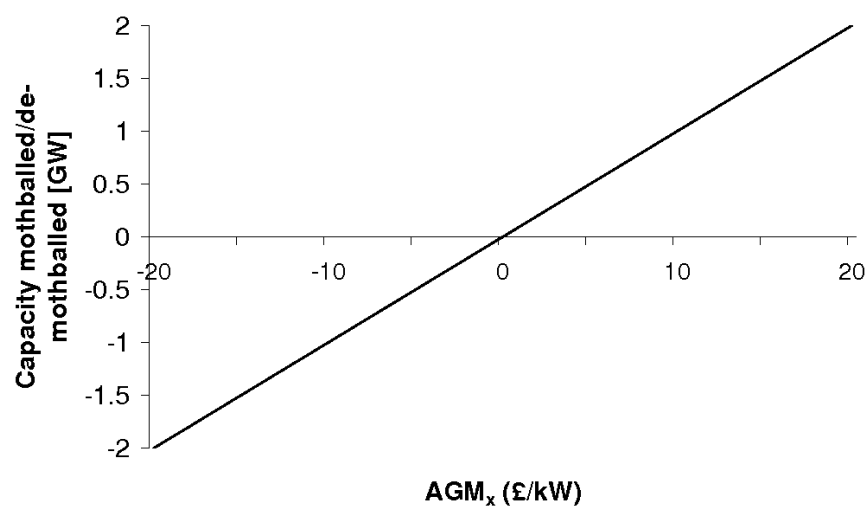


Fig. 3. Plot of model aggregate mothballing response curve. Note that the x-axis has been rescaled to (£/kW).

IV. PRODUCTION COSTING BY MIX OF NORMALS

When estimating expected long-run production costs, there is a need for a reasonably accurate approximation of the load duration curve (LDC). A MOND approximation meets this requirement and is also very easy to convolve with plant outages for the expected output calculations.

A MOND is described as follows: consider a set, $Y = \{y_1, \dots, y_n\}$, of Normally distributed r.v.s. with the i^{th} element having mean μ_i and variance σ_i . Let $\Phi(x|\mu_i, \sigma_i)$ be the cumulative distribution function (cdf) of y_i . A MOND is a convex combination of the Normal distributions and is defined by

$$F(x) = \sum_{i=1}^n p_i \Phi(x|\mu_i, \sigma_i), \quad (11)$$

with $\sum_{i=1}^n p_i = 1$ and $p_i \geq 0$, where p_i is the weight of the component y_i [3]. Let μ and σ be the mean and standard deviation respectively of the cdf described by (11). These parameters have the following properties:

$$\mu = \sum_{i=1}^n p_i \mu_i, \quad (12)$$

$$\sigma^2 = \sum_{i=1}^n p_i (\sigma_i^2 + \mu_i^2) - \mu^2. \quad (13)$$

Another property is that the sum of two variables each distributed as a MOND is itself a MOND. The proof of these properties is in appendix A of [3].

The process starts by splitting the time horizon over which costs are calculated into periods. In this case, the duration of each period is one year; although, shorter periods can also be used to account, e.g., for seasonal capacity. The expected load at each hour is a r.v.

A MOND fit for approximating the annual LDC (MW) is required. For example, if $f_L(x)$ is the probability density function of load and $F_L(x)$ is the cumulative distribution function of $f_L(x)$, then the LDC is simply the rotated and rescaled load *exceedence* distribution.⁵ This is the inverse of $8760(1 - F_L(x))$ where

$$F_L(x) = \sum_{k=1}^K p_k \Phi_k(x|\mu_k, \sigma_k), \quad (14)$$

which is a mixture of K Normals (Φ_k) with the same properties as (11). For a particular K , the best fitting value of each μ_k , σ_k and p_k can be found by solving an optimization problem that minimizes the sum of squares of the difference between observed and fitted values of the LDC.

⁵The exceedence distribution gives $P(X > x)$, that is the probability that the r.v. X (in this case load) is greater than x .

To illustrate the accuracy of this technique at approximating a LDC, Fig. 4 shows the distribution of the GB hourly loads for the period 2005-09 (normalised by the year's average demand) and the fitted distribution. This normalisation is necessary when comparing multiple years to account for demand growth. The difference between the two LDC plots in Fig. 4(b) is not visible at this scale owing to the excellent fit provided by the MOND.

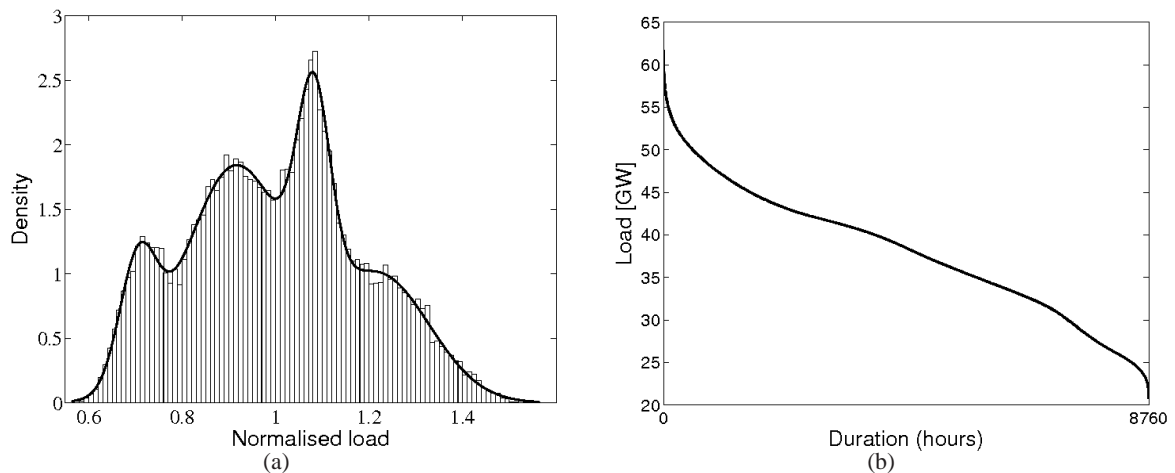


Fig. 4. (a) MOND pdf (4 Normal components clearly visible by their distinct peaks) and histogram of normalised load data and (b) LDC fit with negligible visible difference between mix of 4 Normals and empirical data.

A. MOND with conventional thermal generation (after [3])

The next step is to estimate the available capacity for a set of generating units. The available capacity at each hour from a particular unit is a r.v. which is characterised by the unit's Forced Outage Rate (FOR). Let the capacity of unit u be defined by c_u , its FOR by ρ_u and expected available capacity $G_u = c_u(1 - \rho_u)$. That is, the distribution of the unit's available capacity follows a Bernoulli distribution between zero and c_u ; thus, the unit is either available at full capacity (with probability $1 - \rho_u$) or on full outage with (with probability ρ_u).⁶

If m_u units of type n share the same capacity and FOR characteristics and are subject to independent forced outages, they can be treated as a single pseudo-unit (or generator) with a

⁶More general models exist to account for partial unit outages (e.g., see [25]), however they are not considered here.

distribution with the following moments:

$$E(G_n) = \mu_n = m_u c_u (1 - \rho_u), \quad (15)$$

$$Var(G_n) = \sigma_n^2 = m_u c_u^2 \rho_u (1 - \rho_u), \quad (16)$$

where each (pseudo-) generator, G_n , has capacity $c_n = m_u c_u$.⁷

Now the convolution property of the MOND is used to determine the distribution for the expected load still to be served after each generator is dispatched (in merit order). This distribution is called the *effective load duration curve* (ELDC) facing the next generator to be dispatched [26]. If the units can be grouped into N (pseudo-) generators⁸ each with characteristics (15) and (16), then we can define

$$L_n(x) = P \left\{ L - \sum_{i=1}^n G_i > x \right\} \quad (17)$$

as the load minus the available capacity of generator types $1 \dots n$ ($1 \leq n \leq N$) [3]. If $F_n(x) = 1 - L_n(x)$ is the cumulative probability of effective load $x = L - \sum_{i=1}^n G_i$ facing the $(n+1)^{th}$ generator, then

$$F_n(x) = \int_0^{c_n} F_{n-1}(x+y) f_n(y) dy \quad (18)$$

and

$$L_n(x) = 1 - F_n(x), \quad (19)$$

where $f_n(y)$ is the pdf of the Normal that approximates the Binomial distribution describing the available capacity of the n^{th} type of generation with installed capacity c_n .⁹ $F_n(x)$ is computed by performing the convolution of the Normal distributions for load (which is a MOND) and available capacity.

The convolution property of a MOND [3] is applied, with generator loading carried out by merit order. The expected energy served e_n (in MWh/yr) by generator type n can then be given

⁷To simplify the presentation for the remainder of the paper, the convention will be to use ‘generator’ when referring to a ‘pseudo-unit’ (collection of units of a given type), and c_n when referring to the capacity of that generator, because this is the last time individual units will be discussed.

⁸The more units in a group, the closer the Binomial distribution is to Normal.

⁹Technically for a Normal distribution, the bounds in (18) should be $-\infty$ to ∞ , but it is assumed here that the probability of falling outside the physically possible range $[0, c_n]$ is negligible owing to the Binomial distribution being rescaled to $0/c_u$.

by

$$E[e_n] = 8760 \int_0^\infty [L_{n-1}(x) - L_n(x)] dx, \quad (20)$$

where $L_{n-1}(x)$ is the load still to be met after adding generator type $n-1$ and $L_n(x)$ is the load still to be met after adding generator n , which at the start of the convolution process ($n=0$) is obtained from (14).

The distribution for the ELDC after convolving in n generators is given by:

$$L_n(x) = 1 - \sum_{k=1}^K p_k \Phi_k(x | \mu_{L_k} - \sum_{i=1}^n \mu_{G_i}, \left[\sigma_{L_k}^2 + \sum_{i=1}^n \sigma_{G_i}^2 \right]^{\frac{1}{2}}). \quad (21)$$

Thus, the ELDC is described by a MOND with the same number of component Normals as the original LDC. An example of the iterative convolution process is shown in Fig. 5. The diagram depicts how the remaining expected load to be served is reduced each time a group of generators is convolved with the ELDC.

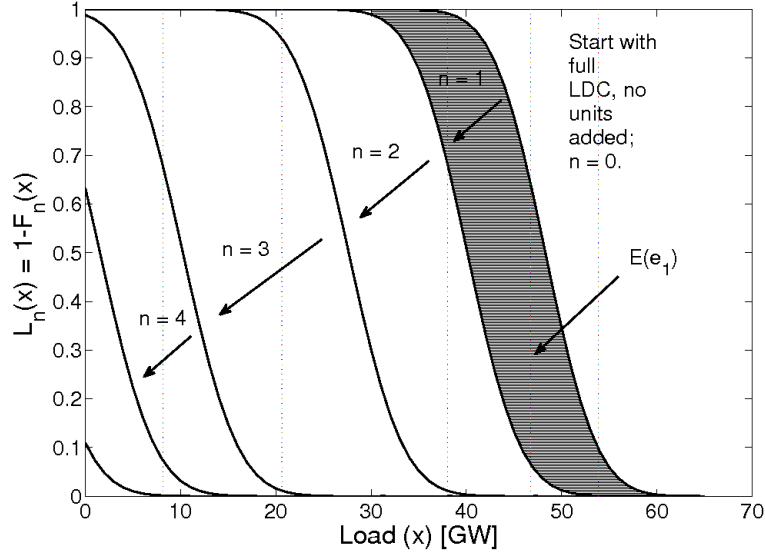


Fig. 5. Example of the convolution process. Shaded region is the expected energy served by the first unit dispatched (i.e., the result of (20) with $n=1$).

Given each $L_n(x)$ ($n=1 \dots N$), the probability that generator n or higher (in the merit order) is the marginal source of energy (and so sets the price) is given by $L_n(0)$, i.e., the point where the function crosses the vertical axis in Fig. 5. Further,

$$h_n = L_{n-1}(0) - L_n(0) \quad (22)$$

is the probability that generator n is on the margin. This result is used in Section IV-C to calculate expected revenues per MW for a generator belonging to this generator type in an ‘energy-only’ market setting.

The unserved energy (MW) is then simply any positive remaining load once all N generators have been added. The annual expected energy unserved (EEU) can be calculated by integrating $L_{N+1}(x)$ (i.e., after convolving in the complete set of N generators) from 0 to ∞ and multiplying by 8760 hrs/yr. Furthermore the Loss-of-Load Expectation (LOLE) for the period is determined by computing $8760 \cdot L_{N+1}(0)$ [25].

B. MOND with a thermal-wind system

Unlike conventional thermal generation units whose individual availabilities are assumed to be independent, wind generators rely on the availability of the “fuel” resource and therefore a dependency between available wind generation at different wind plants is introduced. As a result, the convolution technique used to model thermal generation in [3] cannot be directly used to account for wind power generation.

To address this issue, an exogenous wind capacity is assumed and the resulting residual LDC facing thermal generation is computed and the MOND approximation is applied to this wind-adjusted data set. The residual load is simply the load minus the output from all wind plants at each hour. By taking this approach, the analysis can take into account both spatial correlations and seasonal (e.g., monthly and diurnal) trends in wind availability and their relationship with demand.

It is important to note that the residual LDC approach removes the chronological issues that arise in the wind and load time series. This is particularly important in the presence of large amounts of hydro and pumped hydro generation where chronological production costing methods may be preferred to load duration curve methods. However this implementation of the MOND technique is applied to the GB power system where the amount of hydro and pumped hydro is relatively small (about 4% of capacity), so the use of a load duration curve approach is reasonable.¹⁰

¹⁰Note that there is little scope for new build of hydro technologies in GB due to the lack of suitable sites.

C. Expected revenues from the energy market

In the absence of market power and unless there is a capacity shortage, the market price for energy will equal the marginal cost of the last generator to be dispatched. If there is a capacity shortage, and assuming there is no price cap, the price will clear at the level necessary to ration demand to the available capacity. More precisely, because consumers are not generally exposed to the real-time price, there is a willingness of suppliers (load serving entities in US parlance) to pay up to the Value of Loss Load (VOLL) when there is a shortage.¹¹ This methodology is applied in [4] in a long-run equilibrium model; that approach is extended here to a dynamic long run nonequilibrium setting.

During a particular year, the probability that generator n will be at the margin is given by (22) and the price in that event will be the marginal cost of the generator, MC_n . This assumes price-taking (competitive) behaviour by generators. Furthermore, once the convolution process has been completed for all N generators, the probability that there will be insufficient generation to meet demand is given by $L_{N+1}(0)$ and under this condition the price is assumed to reach VOLL. Using the result in (22), the expected gross margin for a particular MW of capacity belonging to generator n when generator i is at the margin is given by (£/MWh):

$$R_n^i = \max \{h_i(\pi_i - MC_n), 0\} \quad (23)$$

where π_i is the wholesale price when generator i is at the margin, which in the absence of market power is given by MC_i . Using (22) to calculate (23), the expected annual perfectly competitive gross margin (revenue minus variable cost) used in (4) can be calculated by (£/MW/yr):

$$CGM_n = 8760(1 - \rho_n) \left[\sum_{i=1}^N R_n^i + (h_{N+1}(VOLL - MC_n)) \right]. \quad (24)$$

Economists term these ‘‘scarcity rents’’. It is precisely these scarcity rents that, in a simple long-run competitive ‘energy-only’ market model, are just high enough to cover fixed costs and trigger investment [27]. The main numerical work here is in computing the $L_n(x)$ in (20); once these are known, the revenues are calculated easily by multiplying by the price - marginal cost differentials. Note that no start-up or no-load costs are considered here.

It is assumed that in a competitive energy market, generators bid to produce electricity at or around their marginal cost. The rules of the GB market allow for generators to trade freely,

¹¹In a more general case, some or all customers are exposed to the real-time price.

i.e., there is no marginal cost bid rule in place. However this is not a problem because the equilibrium concepts for bilateral and central pool markets have been proved equivalent (see [28] or [29] for the Cournot case). Recent analyses of the GB market [30] showed a tendency for balancing market (BM) prices to rise above the estimated marginal cost of the last generator dispatched in peak demand hours. Other examples of empirical analyses which support this claim include [31, 32]. In [31], an analysis of the Texas BM revealed evidence of bidders, particularly smaller firms, submitting supply curves in excess of their theoretical optimal supply function.¹² [32] found that a Cournot oligopoly model provided a better representation of the California, Pennsylvania-New Jersey-Maryland (PJM) and New England wholesale markets than a perfectly competitive model during peak hours,¹³ and it was during these hours that the presence of price mark-ups was detected. This price mark-up during peak demand hours occurs because firms can raise their bids knowing that the lack of alternative resources will mean their bids will be accepted. In this case the market does not necessarily clear at the marginal cost of production, so in this study price, π , includes an additional mark-up term that alters the shape of the aggregate supply curve as the system approaches scarcity. This new price function is described in [24] and is defined here as:

$$\pi(L, G_1, G_2, \dots, G_N) = mc(L, G_1, G_2, \dots, G_N) + w(L, G_N^*) \quad (25)$$

where $mc(L, G_1, G_2, \dots, G_N)$ is the marginal production cost of meeting the load, L , given realised total available generation $G_N^* = \sum_{i=1}^N G_i$, and $w(L, G_N^*) = ae^{b(L-G_N^*)}$ is a function of the capacity margin, defined as total available capacity minus load in a particular hour (similar to [33]) where L and G_N^* are expressed in GW. Note that the parameters a and b are calibrated so that a capacity margin of zero provides a mark-up equal to the VOLL (e.g., Fig. 7(b)).¹⁴ The use of this function can be justified by comparisons of the GB forward Market Index Price and simulated prices with accurate fuel price data (presented in [24]), however in this example application the parameters used vary slightly. This also agrees with the methodology used in

¹²Profit-maximization where profit function is based on a contract for differences between offer price and cost incurred for supplying contractually obligated and BM quantities.

¹³If vertical arrangements were also accounted for in the PJM and New England case.

¹⁴For instance, for a VOLL of £10,000/MWh, $a = 10,000$ and $b = -1.123$, and for £2,000/MWh, $a = 2,000$ and $b = -1.101$.

[30] to simulate GB system marginal prices where wholesale prices were simulated using a price mark-up function in peak hours.

For simplicity, linear variable costs are assumed for all generators, that is total variable costs are given by $C_n(P) = b_n P$, which leads to a stepped aggregate supply function in the short-run (if bids are assumed to equal generator marginal cost, $MC_n = b_n$) based on the marginal costs of the entire generation set. Fig. 6 shows an example of the price function given by (25); the curve behaves like a classical linear step-wise marginal cost supply function for small loads, but as the system approaches scarcity, the mark-up function becomes evident and soon dominates the pricing mechanism.

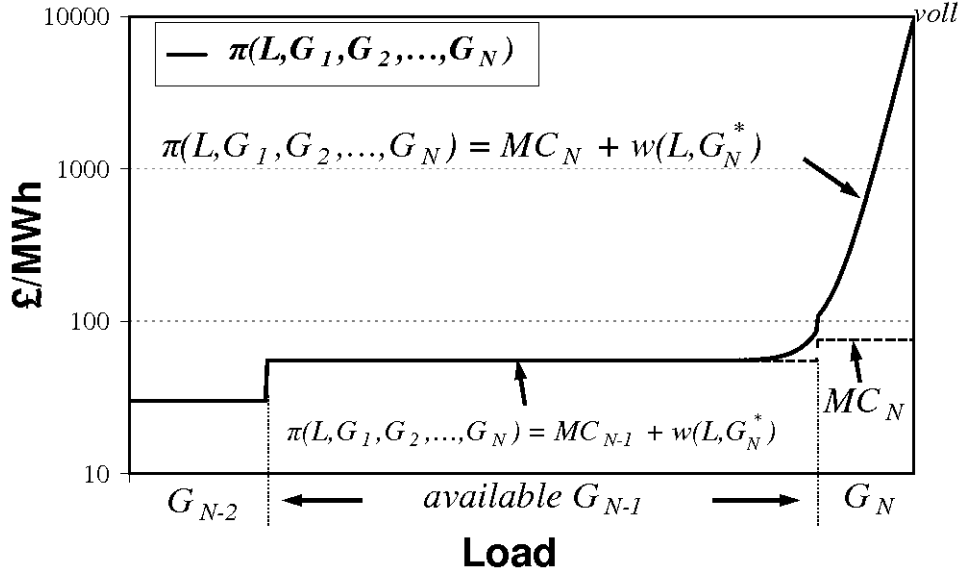


Fig. 6. Supply function for a given realised available capacity for generators $N - 2$, $N - 1$ and N with mark-up function defined by $w(L, G_N^*) = ae^{b(L-G_N^*)}$ (shown as black line). Marginal cost dashed, price is solid line.

Now the market price (25) no longer just depends on which generator is on the margin, which is the case under the classic perfectly competitive market case (24); it now depends on the overall margin, $G_N^* - L$ as well. Furthermore, since the price can exceed MC_n if n is on the margin, the question of whether a particular incremental MW of capacity within n is called upon or not must be considered. This is because marginal generator n can still earn a positive gross margin.

If R_n^{L, G_N^*} is the gross margin received by a MW of capacity from generator n for load L and total available generation G_N^* , then R_n^{L, G_N^*} will be calculated by one of the following means:

- 1) If the marginal generator, say i , is below n in the merit order (i.e., has a lower marginal cost) then the generator n will not be dispatched and $R_n^{L, G_N^*} = 0$.¹⁵
- 2) Else if the marginal generator has a higher marginal cost than n , then the probability of dispatch is 1 and $R_n^{L, G_N^*} = mc(L, G_1, G_2, \dots, G_N) + w(L, G_N^*) - MC_n$.
- 3) Else if n is the marginal generator, then the probability of dispatch is between 0 and 1 and

$$\begin{aligned} R_n^{L, G_N^*} &= mc(L, G_1, G_2, \dots, G_N) + w(L, G_N^*) p_n^{disp} - MC_n \\ &= w(L, G_N^*) p_n^{disp}, \end{aligned} \quad (26)$$

where p_n^{disp} is the probability that a MW belonging to generator n is dispatched.

This probability of dispatch is approximated by

$$p_n^{disp} = \max \left(\min \left\{ 1, \frac{-M_{n-1}}{c_n(1 - \rho_n)} \right\}, 0 \right), \quad (27)$$

where $M_{n-1} = \sum_{i=1}^{n-1} G_i - L$ is the surplus margin after L has been met using all available generation lower in the merit order than n (e.g., Fig. 7). In plain terms, (27) is the ratio of the MWs of generator n that are dispatched to the average total MW of n that are available (which will differ from the actual available MWs of n in any particular realisation). In the event that this margin is negative, the fractional term in (27) will be greater than 1, therefore the $\min \{ _ \}$ function is required in order to eliminate this possibility. This method of calculating dispatch probabilities is required to account for market price mark-up (25).

The expected gross margin (24) must now be extended to consider the price function (25) and merit order operation. This is less straight-forward than under marginal cost-based pricing (23) because the market price mark-up requires consideration of the total (generation-load) margin, M_N , as well as the marginal unit.

By assuming that price mark-up is non-zero (i.e., $w(L, G_N^*) > 0$) only when generator N or $N-1$ is on the margin, calculation of the probability distribution of $w(L, G_N^*)$ can be achieved by considering the joint probability distribution of just the capacity margins M_{N-1} and M_N . This assumption is reasonable in an aggregated capacity model where the generator size is large. What's more, empirical evidence from the GB market (e.g., [30]) is that mark-up tends to occur

¹⁵Thus we are assuming for simplicity that dispatch is still in merit order, despite the presence of market power. However, in oligopolies with asymmetric generating companies, a small high cost generator might produce power before a large low cost generator, as the latter is more likely to withhold capacity. This possibility is not considered here.

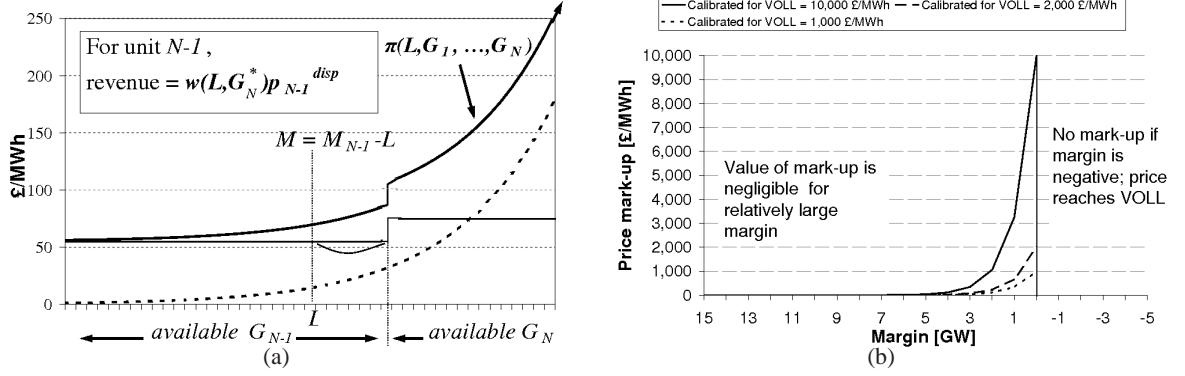


Fig. 7. (a) Aggregate supply curve showing price (solid upper line) for load L and revenue for generator of type $N - 1$. mark-up function also shown (dashed line). (b) Shows price mark-up for different values of capacity margin and calibrations for $a = 10,000, 2,000$ and $1,000$.

predominately during peak periods when surplus margins are relatively small, and the surplus of available resource in other periods means the presence of market power is unlikely. Therefore, it is reasonable to assume that price mark-up is significant only when peaking plants N or $N - 1$ are on the margin.

D. Expected price mark-up calculation

Firstly, for each component of the MOND (11), we consider the joint distribution of capacity margins M_{N-1} and M_N , which is given by $f(M_{N-1}, M_N)$. The correlation is calculated as:

$$\begin{aligned}
 \text{corr}(M_N, M_{N-1}) &= \frac{\text{cov}(M_N, M_{N-1})}{\sigma_{M_{N-1}} \sigma_{M_N}} \\
 &= \frac{\sigma_{M_{N-1}}^2}{\sigma_{M_{N-1}} \sigma_{M_N}} \\
 &= \frac{\sigma_{M_{N-1}}}{\sigma_{M_N}}.
 \end{aligned} \tag{28}$$

This can be proved by considering the correlation between $X + Y$ and X , where X and Y are independent variables, then

$$\begin{aligned}
\text{corr}(X + Y, X) &= \frac{\text{cov}(X+Y, X)}{\sqrt{\text{Var}(X+Y) \cdot \text{Var}(X)}} \\
&= \frac{E((X+Y) - [E(X)+E(Y)]) \cdot (X - E(X))}{\text{sqrtVar}(X+Y) \cdot \text{Var}(X)} \\
&= \frac{E((X - E(X)) + [Y - E(Y)]) \cdot (X - E(X))}{\sqrt{\text{Var}(X+Y) \cdot \text{Var}(X)}} \\
&= \frac{E[(X - E(X)) \cdot (X - E(X)) + [Y - E(Y)] \cdot (X - E(X))]}{\sqrt{\text{Var}(X+Y) \cdot \text{Var}(X)}} \\
&= \frac{\text{Var}(X) + 0}{\sqrt{\text{Var}(X+Y) \cdot \text{Var}(X)}} \\
&= \sqrt{\frac{\text{Var}(X)}{\text{Var}(X+Y)}}.
\end{aligned} \tag{29}$$

Fig. 8 shows a plot of the isoquants of the bivariate Normal density for $\{M_{N-1}, M_N\}$, which are highly positively correlated owing to increases in M_{N-1} increasing M_N . For a particular point (M_{N-1}, M_N) , the diagram shows the value of the joint pdf (ellipses) and price mark-up isoquants (dotted lines in each quadrant centred $(0, 0)$). By splitting the space into four quadrants and sketching the isoquant maps, the effect of available capacity margins on plant revenues can be assessed. For instance, when plant type N is not dispatched (north-east quadrant), increases in M_N result in a decrease in mark-up (indicated by parallel horizontal lines, two example mark-ups shown). Likewise, when N is dispatched (north-west quadrant, M_{N-1} is in shortage). If M_N is in shortage (south-west quadrant), the mark-up is zero for all combinations M_N and M_{N-1} (i.e., system is short of resource and the price will reach the VOLL). Note that the south-east quadrant is assumed to have zero probability; it would be calculated as having a nonzero probability only because the Normal approximation will give an unrealistic nonzero probability for negative availability capacity for generator $N - 1$. However, in the application, this probability is negligible.

Next, for each component of the MOND (11), the revenue that a MW belonging to generator $n \leq N$ earns from price mark-up, RPM_n (£/MWh), is considered for the following cases:

- 1) If $n < N - 1$ (i.e., lower in merit order than $N - 1$), then the expected revenue from price mark-up for a particular MW of that capacity is given by

$$RPM_n = \int_0^v (1 - \rho_n) f(M_N) w(M_N) dM_N, \tag{30}$$

where $f(M)$ is the pdf of the surplus margin $M_N = G_N^* - L$. This assumes that $w(M_N)$ is a function of M_N only, i.e., the overall system margin, and that generators $N - 2$ and

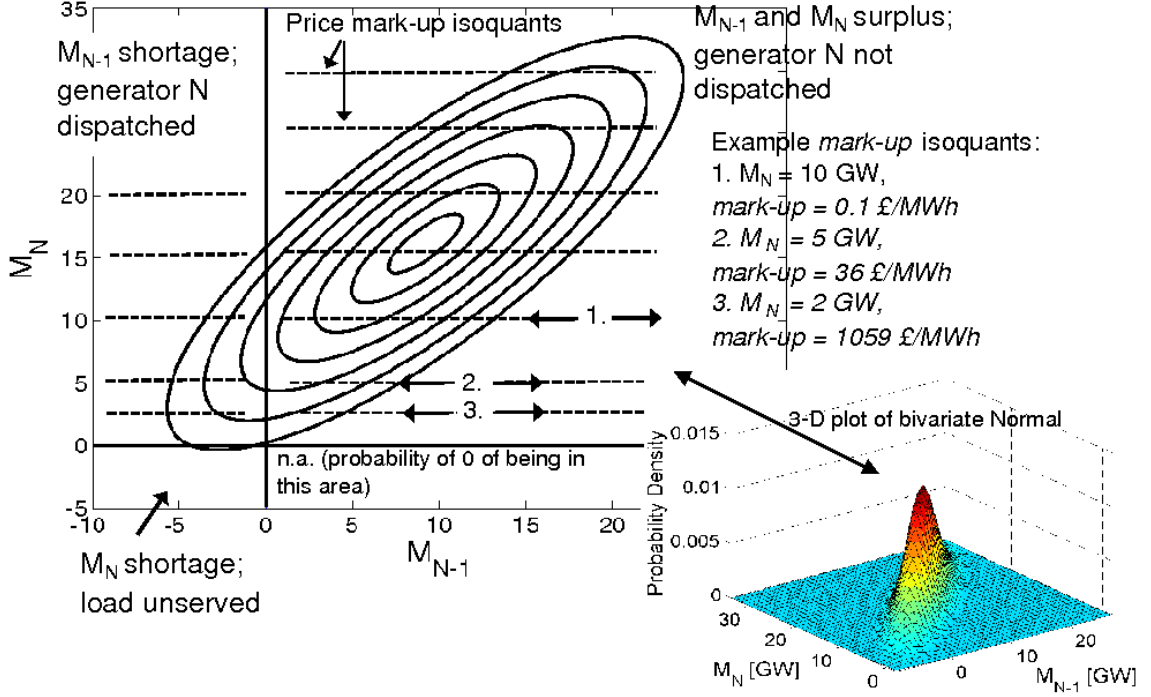


Fig. 8. Diagram showing 3-D plot of bivariate Normal of $\{M_{N-1}, M_N\}$ (right) and its image on a 2-D plane (left) with isoquant maps for the price *markup* element of (25).

$N - 3$, etc are all fully dispatched when mark-up is nonzero. The integral lower bound in (30) is zero due to price mark-up being zero if $M_N < 0$. More precisely, if the overall margin is negative then there is no mark-up and the price is set by the marginal cost of demand (i.e., VOLL). The integral upper bound in (30) is some value, v , above which the price mark-up is negligible owing to the large surplus margin (e.g., 7 GW in Fig. 7(b)).

2) Else if $n = N - 1$, then RPM_n is broken down into two sub-cases:

a) If $M_{N-1} \leq 0$ (i.e., north- or south-west quadrant of Fig. 8) then

$$RPM_n = \int_{-\infty}^0 \int_0^v (1 - \rho_n) f(M_N, M_{N-1}) w(M_N) dM_N dM_{N-1}, \quad (31)$$

which is the case where all of generator $N - 1$'s available capacity will be dispatched because load exceeds the available capacity of generators 1 through $N - 1$. Again, the inner integral lower bound is 0 because $M_N \leq 0$ results in zero price mark-up (south-west quadrant of Fig. 8).

b) Else if $M_{N-1} > 0$ (which implies $M_N > 0$, so north-east quadrant of Fig. 8)¹⁶ then

$$RPM_n = \int_0^v \int_{M_{N-1}}^v p_{N-1}^{disp} f(M_N, M_{N-1}) w(M_N) dM_N dM_{N-1}, \quad (32)$$

where p_{N-1}^{disp} is the probability of dispatch of generator $N - 1$, given by:

$$p_{N-1}^{disp} = \frac{(1 - \rho_{N-1})M_{N-2}}{-1 \cdot (M_{N-1} - M_{N-2})} \quad (33)$$

where M_{N-2} is the surplus margin after all available generation lower in the merit order than $N - 1$ has been dispatched.¹⁷ M_{N-2} is a r.v. and computation of its pdf is awkward; however it can be approximated as follows: $M_{N-2} \approx (E(G_{N-1}) - M_{N-1})$.

This is achieved by approximating the realised value of G_{N-1} by its expectation, (15): $E(G_{N-1}) = c_{N-1}(1 - \rho_{N-1})$.¹⁸ Leading to:

$$p_{N-1}^{disp} \approx \frac{(1 - \rho_{N-1})(c_{N-1}(1 - \rho_{N-1}) - M_{N-1})}{-1 \cdot (M_{N-1} - (c_{N-1}(1 - \rho_{N-1}) - M_{N-1}))}, \quad (34)$$

i.e., the expected surplus margin over generator n 's expected available capacity. Note that $M_{N-1} > 0$, so $M_{N-2} < 0$,¹⁹ and thus $0 < p_{N-1}^{disp} < 1$.

3) Else $n = N$ and $M_{N-1} < 0$ and $M_N > 0$ (i.e., north-west quadrant of Fig. 8).²⁰

$$RPM_n = \int_{-\infty}^0 \int_0^v p_N^{disp} f(M_N, M_{N-1}) w(M_N) dM_N dM_{N-1}, \quad (35)$$

where

$$p_N^{disp} = \frac{(1 - \rho_N)M_{N-1}}{-1 \cdot (M_N - M_{N-1})}, \quad (36)$$

i.e., the case where M_{N-1} is in shortage and some volume of capacity from generator n ($= N$) will be required to meet L .²¹

¹⁶We assume that the probability of being in the south-east quadrant of Fig. 8 is zero because of the discussion above.

¹⁷The -1 scalar is applied to the denominator of (33) in account of M_{N-2} being negative. If it was positive, then G_{N-1} would not be dispatched (i.e., $p_{N-1}^{disp} = 0$), which is not considered in (32).

¹⁸Note here that c_{N-1} is the capacity of the generator type $N - 1$, which is the sum of a number of individual units who share the same capacity and FOR characteristics (see footnote 7).

¹⁹In general, M_{N-2} could be positive, however the assumption here is that it is negative when price mark-up is greater than zero.

²⁰There is no second case here; only the case where $M_{N-1} < 0$ is of interest (if $M_{N-1} > 0$ then G_N is not dispatched and mark-up revenue is zero).

²¹The pdf of capacity margin is Normal in account of both available generation and load (in fact, a MOND) being Normal. Therefore M_{N-1} and M_N could conceivably be $-\infty$. However, practically speaking the outer integral lower bound in (31) and (35) is set to $-1 \cdot [\text{maximum value of load}]$ (i.e., the highly unlikely situation when all generation is unavailable).

Finally, by integrating over the subregions of the $\{M_{N-1}, M_N\}$ space in Fig. 8 (i.e., using cases 1-3 above), the expected annual gross margin for generator n can be calculated as

$$GM_n = CGM_n + E[e_n] \cdot RPM_n. \quad (37)$$

This is repeated for each component of the MOND.

This is an important extension to (24); by exploiting the properties of the probability distribution of capacity margins, this allows for the additional revenue received from market price mark-up to be calculated during the production costing process. Procedures for calculating price mark-ups in probabilistic production costing models have been proposed (e.g., see [34] where a Cournot model is proposed). To our knowledge this is the first time these derivations have been presented.

To speed up the computation of (31)-(35), the outer integral is carried out using Gaussian quadrature (GQ), which requires fewer function evaluations than other methods, such as the recursive adaptive Simpson quadrature and is given by

$$\int_{-1}^1 f(x)dx \approx \sum_{i=1}^n w_i f(x_i) \quad (38)$$

which after some manipulations, can be applied to the interval $[a, b]$. Here $n = 100$ is used.

E. Test of accuracy

To test the accuracy of this method, the results of a Monte Carlo (MC) simulation were compared with the MOND technique. That is, for the load (a MOND) and generator cost inputs given in Table I, capacity mix given in Table III and mark-up function calibrated to VOLL 10,000 £/MWh, random samples for load and generator availability were taken. Using these samples, the margin, M_N , price (25), and energy market gross margins were calculated for each unit. Close attention was paid to the tail of the distribution by using importance sampling. More precisely, high loads were oversampled using the component Normal of the MOND with the largest mean (i.e., row 1 in Table I) with corresponding mean μ_1 , standard deviation σ_1 , and pdf $f^*(x)$. Samples were then weighted using the weighting function $W(x) = f(x)/f^*(x)$, where $f(x)$ is the 4 component MOND pdf and x is the random sample from $N(\mu_1, \sigma_1^2)$.

The MC simulation was repeated 10^6 times. The results of this test are displayed in Table II. ‘‘MOND’’ shows the results for the MOND technique including the methods and approximations

of Section IV, above. “Monte Carlo” is for a Monte Carlo (MC) test where available capacity is sampled from a Normal distribution with parameters defined by (15)-(16). Finally, “Bernoulli” samples available capacity from a Bernoulli distribution (i.e., 0 or full capacity based on uniform random number generation for given FORs). The Bernoulli test makes no approximations concerning the distribution of available capacity or its effects on prices and mark-up, and so is the standard against which the new MOND model should be compared. Comparing the MOND and Bernoulli tests shows the effect of using a Normal approximation for available capacity rather than the Bernoulli distribution. Encouragingly the MOND technique matched quite well to the MC simulation (with only a mild over-estimation of gross margins by the MOND technique). Further, the Normal approximation for available capacity also performs well. This test gives confidence that the MOND approximation is a good one. Note that the “energy expected per generator” in Table II for the Monte Carlo and Bernoulli tests is the result of multiplying the mean utilisation across the MC runs of each generator by the total theoretical available energy of each generator. For instance, if the capacity of generator $N - 3$ is 11 GW and the mean utilisation is, say 0.75, then energy expected is given by $8760 \times 11 \times 0.75 = 72,270$ GWh. For the MOND test, this is calculated using (20).

TABLE I
INPUTS FOR MOND TEST CASE.

Loads (MOND)	μ_i (MW)	σ_i (MW)	p_i	
	43802	5743	0.43	
	41650	1410	0.12	
	33971	3372	0.33	
	26089	1771	0.12	
	$N - 3$	$N - 2$	$N - 1$	N
Generator MCs (£/MWh)	7	40	45	60

V. CASE STUDY ASSUMPTIONS

The new dynamic model is applied to an ‘energy-only’ market in which there is no separate capacity market, setting with a initial capacity mix comparable to the GB power system and a

TABLE II
SUMMARY OF RESULTS FOR MONTE CARLO TEST.

	Scarcity rent (£/MWh)				Price mark-up (£/MWh)				Energy expected per generator (TWh)			
	$N - 3$	$N - 2$	$N - 1$	N	$N - 3$	$N - 2$	$N - 1$	N	$N - 3$	$N - 2$	$N - 1$	N
MOND	1.48	1.70	1.70	1.36	39.03	6.03	2.15	2.05	72.27	198.89	63.12	0.12
Monte Carlo	1.43	1.64	1.66	1.33	38.96	5.96	2.09	1.99	72.24	198.88	63.09	0.12
Bernoulli	1.41	1.61	1.63	1.30	38.91	5.92	2.04	1.94	72.24	199.40	63.11	0.12

VOLL of £10,000/MWh with a simulation time horizon of 30 years (2010-40). To reflect the restrictions in suitable sites for nuclear builds in GB, total installed nuclear capacity is constrained to 30 GW.

The expected hourly aggregated onshore wind output in GB is simulated using the methodology described in [35] by obtaining GB wind speed data for 2005-09 (to match the empirical load data), transforming to capacity factors using a Vestas V80-2 MW wind turbine power curve and applying regional weightings derived from the current wind capacity in operation, construction, or consented in GB.

For offshore wind, the expected hourly aggregated capacity factors are calculated using the simulated wind speeds from the Weather Research Forecast Model developed at the University of Edinburgh [36]. This is a fully compressible, nonhydrostatic mesoscale atmospheric 3km grid point model similar to the Met Office Unified Model [37]. It has been validated against measured offshore wind speed data for a number of sites [38], and in the absence of extensive measurement data, provides credible estimates in time and space for the GB offshore wind resource. The wind speeds are transformed to capacity factor using the same approach as [35] using the larger Vestas V90-3 MW power curve. The weighted regional capacity factors are based on the results from the GB 1-3 Crown Estate Round auctions [39].

The total installed wind capacity is exogenous to the model, and is expected to increase linearly from 2010 levels up to 30 GW by 2020 with a maximum of 35 GW in 2025, after which it levels off. We justify this approach by the fact that, to date, large-scale investment in wind capacity is driven by political, rather than economical considerations. It is therefore assumed that policies

promoting investment in wind generation are successful in meeting renewables targets,²² and the purpose of this work is to provide insights into the response of investment in thermal generation and subsequent levels of security of supply risk. The allocation between onshore and offshore areas is consistent with the data in [35] and [39].

The residual load facing thermal units for a particular hour is calculated by scaling the hourly wind production by the installed capacity and subtracting it from the full load. Fig. 9 shows an example of the impact on the 2005-09 residual load histograms as penetration of wind increases. Each of the 30 year's MOND residual load curves are precalculated assuming fixed underlying demand patterns and are then scaled over time in order to match the load growth assumptions.

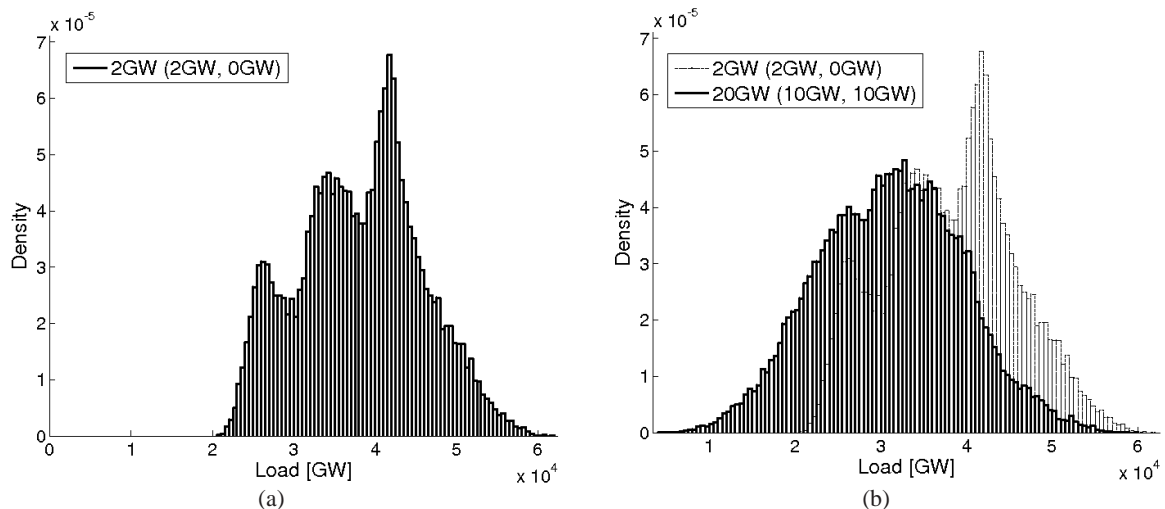


Fig. 9. Result of increasing installed wind capacity from (a) 2 GW to (b) 20 GW on residual load histograms. Data shown is for 2005-09. Numbers in brackets indicate volume of onshore and offshore capacity respectively.

Data on initial 2010 system capacity in Table III is derived by aggregating GB capacity data [41] into the five capacity types and unit sizes described in Section II. To keep the model simple, minor sources of peaking capacity such as oil and pumped storage is combined with OCGT. CHP and hydro are aggregated with CCGT plant to obtain the unit totals shown in Table III. To reflect capacity already under construction in GB, 10.7 GW of CCGT capacity is assumed to come online during the first (1.5 GW), second (5 GW) and third (4.2 GW) years of the simulation.

²²For instance, the UK Government has a target of around 30% renewable electricity generation by 2020 in order to meet the binding European Union target for renewable energy [40].

TABLE III
GENERATOR INPUT ASSUMPTIONS WITH SYMBOLS DEFINED IN SECTION III.

Technology x	Therm. eff.	FOR ρ	Capex £/kW	FC £/kW/yr	Var. O&M £/MWh	Lifetime α (yrs)	Build τ (yrs)	WACC r (real) ^a	$T AFC$ £/unfor.MW/yr	$TIAC$ £/MW	Initial (GW)	No. units
Nuclear	0.36	0.10 ^b	2,913	37.5	1.8	40	7	0.09	400,750	931,170	11	22
Coal	0.35	0.14	1,789	38.0	2.0	40	5	0.07	216,710	344,100	27.5	55
CCGT	0.53	0.13	718	15.0	2.2	25	3	0.07	91,840	96,030	28.6	143
OCGT	0.39	0.10	359	15.0	4.4	40	2	0.07	47,250	36,690	7.7	154

^aAssuming a 2.5% rate of inflation. ^bRecent years have shown a decline in the annual availability of the GB nuclear fleet (likely due to age), therefore this value is reduced to 75% for existing nuclear capacity. New nuclear builds are expected to have 90% availability.

Existing plant included in the Large Combustion Plant Directive (LCPD)²³ is modelled with a reduced lifetime based on the estimates of remaining generating hours given in [42]. All other existing units are given retirement dates consistent with the lifetime assumptions in Table III. This table also shows the financial and technology input assumptions, including capacity cost assumptions, $T AFC_x$ and $TIAC_x$ (cf. Section III-A).

We assume there will be no load growth until 2020 (although, as explained, realised growth varies around the mean rate). This is broadly in line with central Updated Energy Projections published by DECC [43] and base forecast winter peak demand figures from the GB System Operator (SO) [41]. Expected electricity demand after this point is assumed to grow at 1% per year until 2025, after which it levels off.²⁴

Exchange rates are assumed to remain constant at €1.20/£ and \$1.50/£. All calculations are carried out in real pounds sterling. Real discount rates are used owing to the forward estimates for fuel and carbon prices being in real terms. All capital and operating costs are constant in real terms (2008 prices).

²³A control on emissions from heavily polluting large combustion plant introduced by the European Union in 2001. Approximately 11 GW of emission-intensive capacity is expected to be decommissioned by 2016 under this legislation

²⁴Note that the DECC projections do not go beyond 2025 and the GB SO planning timescale is up to 7 winters ahead.

VI. CASE STUDY RESULTS

A. Base case results

The model has been implemented using in the Matlab/Simulink environment. For a GQ (38) with 100 points, the computational efficiency of the MOND technique allowed for each production costing run to execute in under 1.5 seconds. Thus the 7 stochastically simulated years and 100 MC simulations required $7 \times 100 \times 2 = 1400$ seconds. Consequently, for the 30 year simulation, execution took between 525 and 1575 minutes, depending on the number of technologies chosen for investment (recall the iterative characteristic described in Section III-C).²⁵

Fig. 10(b) shows the evolution of total installed capacity in the simulation. New builds and plant retirements are shown in Fig. 11(a) along with the evolution of the mix and amount of generation over time in Fig. 11(b). Shown in Fig. 10(a) is the full and de-rated capacity margin. The de-rated margin is the ratio of de-rated capacity (DC) (installed capacity scaled by expected availability at peak demand) to most probable peak load (PL); i.e., $[DC]/[PL] - 1$. The forecast for PL is obtained from the 99.9% percentile of the year's MOND cdf for full load (i.e., the load which is exceeded approximately 9 hours per year). The FORs in Table III are used to de-rate conventional capacity, and for wind the long-term capacity credit (%) values are calculated using only those hours within 10% of peak demand [35]; these range from 9-35% depending on level of installed capacity (the higher the total installed capacity, the lower the capacity credit). These capacity credits provide an estimate of the expected contribution of wind generation to supporting peak demand.²⁶ Furthermore the use of de-rated margin permits the level of security of supply risk to be estimated when high penetrations of wind generation are present and calculation of an absolute level of risk is difficult. Moreover it can easily be compared with the GB SO's current estimate of what constitutes an acceptable margin.²⁷

To compare the performance of the simulation against historic trends in GB, the model was run from 2001-10 and a comparison between the modelled and actual capacity margins was

²⁵Plainly, reducing the number of GQ points shortens the production costing execution time (e.g., 25 points provided a 0.7 second saving), however the accuracy of the MOND technique shown in Table II decreases.

²⁶Periods of highest demand are typically associated with at least some wind [44].

²⁷For example, see Appendix to [42] and the UK Government's recent consultation on GB electricity market reform [40].

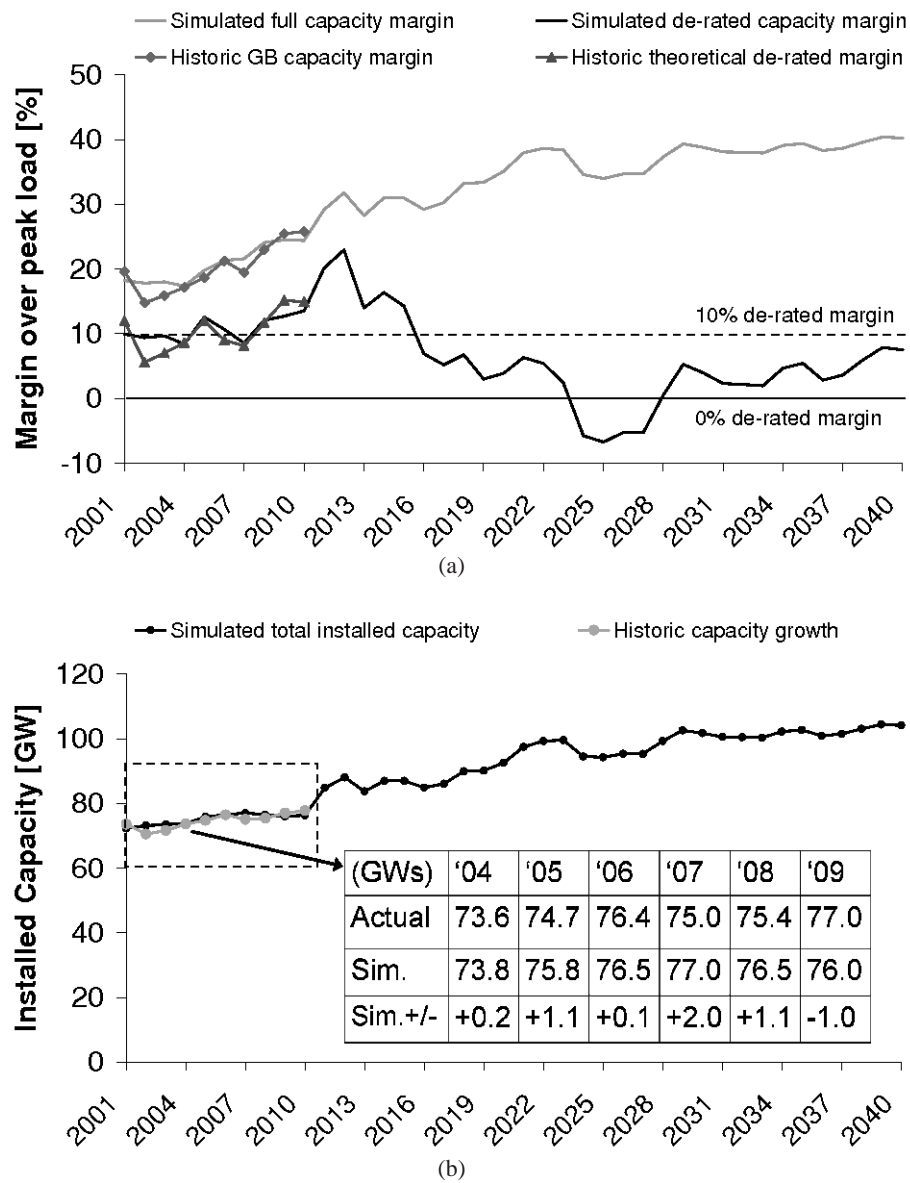


Fig. 10. (a) Plot of simulated de-rated and full capacity margins. Historic theoretical GB capacity margins (2001-10) derived using data from [42] and [45]. (b) Plot of simulated capacity growth. Historic 'actual' capacity (2001-10) derived using data from GB SO's Winter Outlook reports [42].

performed.²⁸ The comparison shows that simulated margins do not perfectly match historic trends in all years (e.g., 2002/3), however there is a reasonably good agreement of our model with reality, which gives a degree of confidence in the realism of our future projections. Note

²⁸See [24] for cost and initial capacity data.

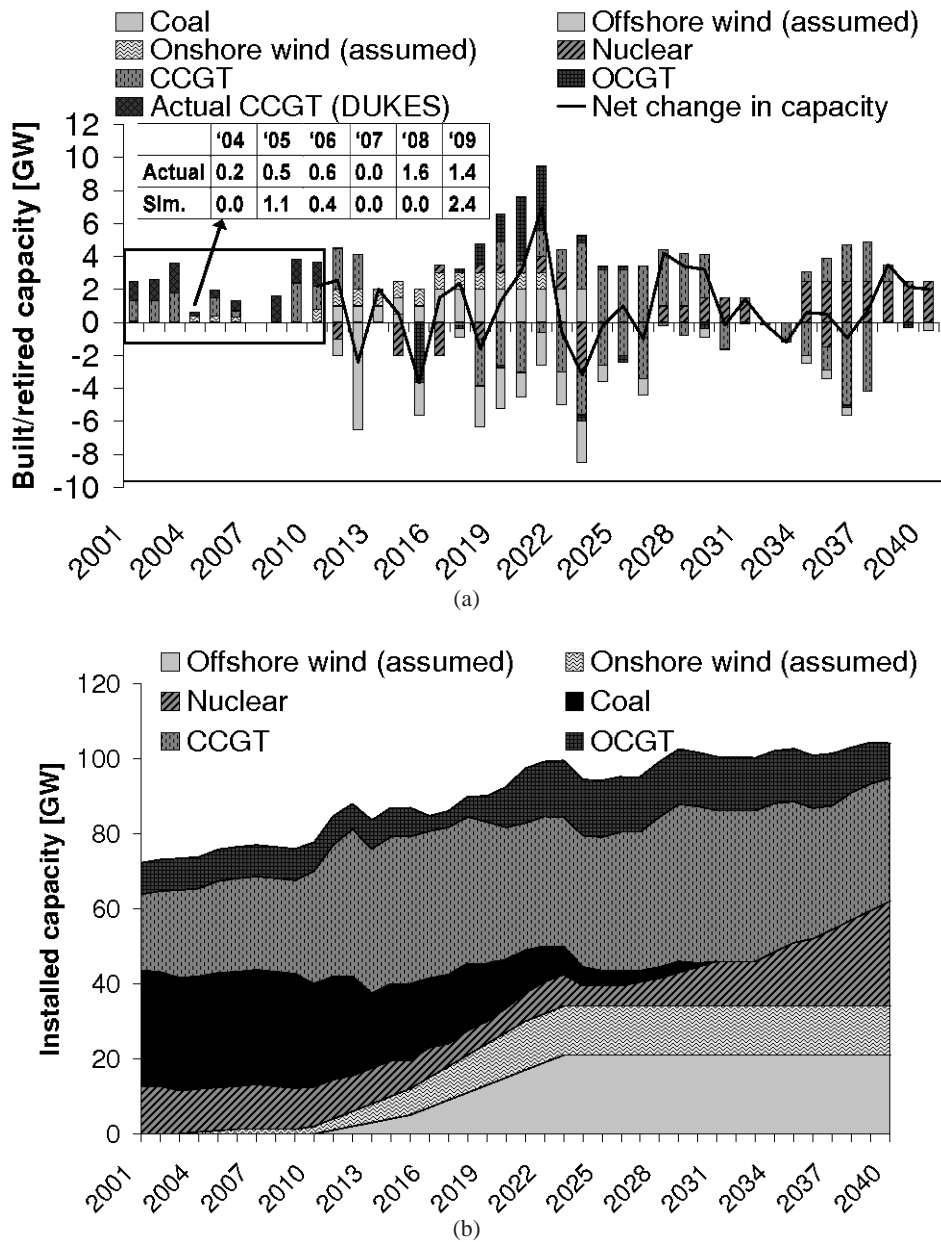


Fig. 11. (a) Plot of simulated new builds and retirements over time. Negative bars indicate plant retirements and positive bars indicate new builds. Also shown are historic new builds (all CCGT) for 2001-09 (columns labelled 'CCGT DUKES' [46]). (b) Plot of total installed capacity over time, i.e., the result of the mix and amount of generation investment and retirements over time.

that the “historical theoretical de-rated margin” is what the forecast de-rated margin would have been for a given winter using the assumptions about plant availability and winter peak load. This data can be obtained from the GB SO’s Winter Outlook reports (e.g., [42]). Furthermore,

the comparison of available historical data on capacity additions plotted in Fig. 11(a) shows that the CCGT investments triggered by the simulation (columns after 2003) do not correspond in all years (e.g., 2008) but the volumes and timing are not unreasonably different.

The future trend shows an erosion of de-rated capacity margins after around 2015. This coincides with the LCPD plant retirements and rapid offshore wind growth. Of the 30 simulated future years, the average de-rated margin is 5.6% with a standard deviation of 7.1%. De-rated margins are negative in 4 years, below 5% in 15 years, and below 10% in 25 years. For those years where margins are below 10%, an average shortfall of 1 GW of capacity was projected. The UK Government's recent consultation and subsequent white paper (July 2011) on GB electricity market reform has stipulated that a peak de-rated margin of 10% provides an acceptable level of generation adequacy risk [40]. Further, the GB SO has recently stipulated that a de-rated capacity margin of 5 GW over expected peak demand is desirable (see Appendix to [42]). These simulation results suggest that a lower than desirable level of adequacy risk could potentially occur.

The annual LOLE and EEU was also calculated (cf. Section IV-A). The average annual LOLE across the 30-year simulation was 0.03 hrs/yr with a standard deviation of 0.05, and average annual EEU of 5.7 GWh (less than 0.002% of typical year's total annual energy demand). The yearly LOLE together with the volume of hypothetical additional capacity required to meet a 5 GW de-rated capacity margin at peak is plotted in Fig. 12.²⁹ The graph shows how the LOLE is higher in some years, particularly in 2023-26, which is reflected in the de-rated peak margin shortfall. To put these figures in context, an historic generation adequacy risk calculation is required; this will allow performance relative to historic levels of risk to be assessed. However this analysis is beyond the scope of this paper. Further, the MOND representation is less accurate for the tails of the distribution and so these risk indices should be interpreted with caution. With this in mind, the values for LOLE and EEU are used primarily to assess the changes in relative levels of risk over the simulation time horizon and to benchmark the sensitivity analyses described below rather than to predict absolute levels of system risk.

These projected risk and de-rated capacity margin figures suggest that the system may experience tight supply conditions during peak demand in some years. Some of these results can

²⁹A value of zero implies that de-rated margin is in excess of 5 GW.

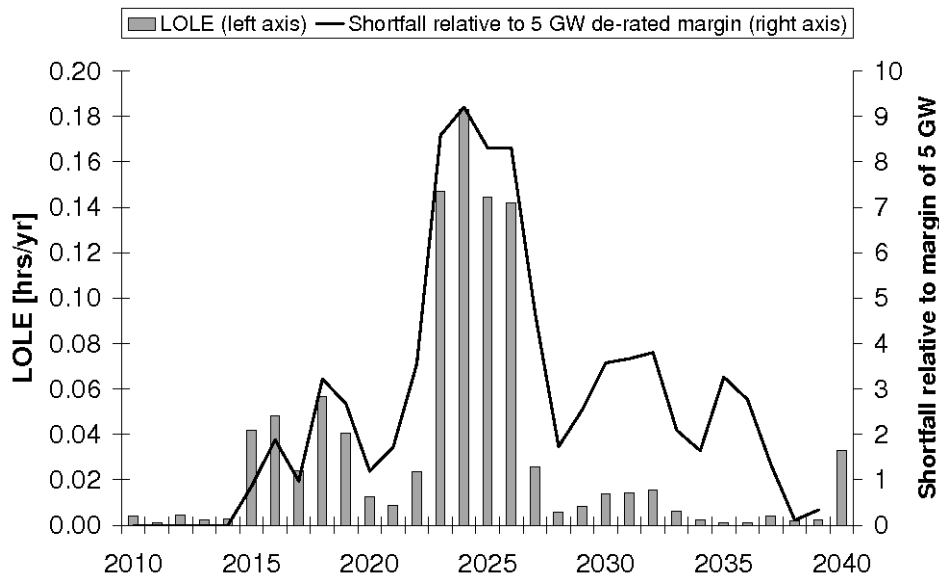


Fig. 12. Plot of simulated LOLE (bars) and capacity shortfall over 5 GW de-rated capacity margin (solid line).

perhaps be explained by inspection of the residual load histograms from Fig. 9(b); the shape of the right-most tail suggests that even with very high penetrations, wind power does not contribute in all high demands periods. However the frequency of these high-demand/low-wind periods is too low to justify investment by private investors. And it is these very high-demand hours when the potential for a capacity shortfall is highest (excluding here SO actions such as voltage reductions). From a policy perspective, it is arguably uneconomical to design policies aimed at ensuring there is adequate generating resource available for these low-frequency events; an alternative approach would be to encourage demand-side participation through smart grids and smart metering. However these mechanisms will introduce price dynamics not currently witnessed in most liberalised energy markets and therefore careful consideration of the impact of demand response on generator's anticipated energy market revenues is required. However this consideration is beyond the scope of our investigation.

Further, an analysis of generator revenues shows symptoms of a boom and bust investment cycle. Simulated OCGT total gross margins, which include annualised capital costs (cf. Table III), are plotted in Fig. 13. Also shown are the triggered investments in this technology. Recall here that investors stochastically simulate 7 years of prices, so the largest investment years (2017/18) include the forecast prices for (2023-25), the period when gross margins are highest. However

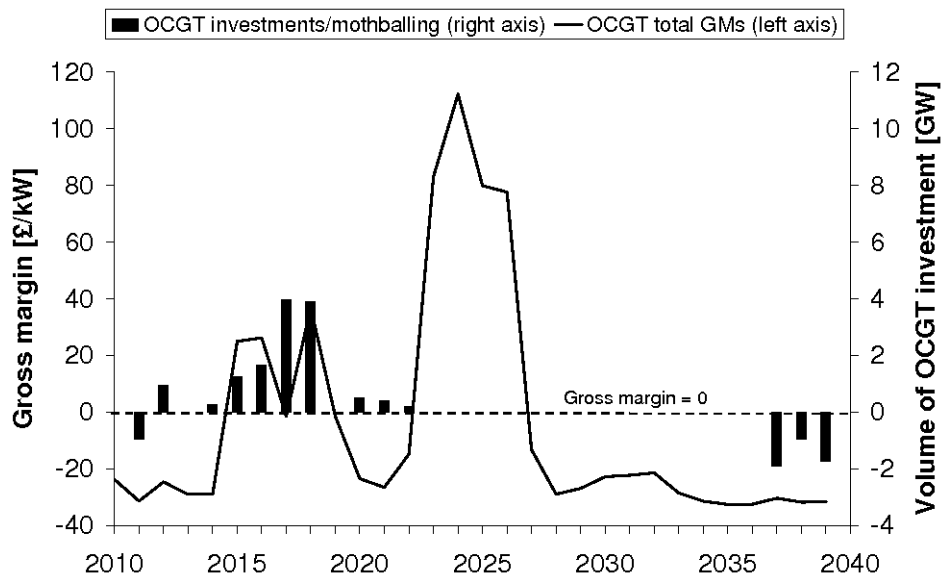


Fig. 13. Plot of simulated total gross margins for OCGT capacity (solid line, left axis). Also shown are the OCGT investment and mothballing amounts over time (black bars, right axis).

investment reduces in 2019-22 in response to expectations about prices being dampened (although not sufficiently to prevent an overshoot) as new investment in OCGT and other technologies enter the system. It is easy to see the pattern of high gross margins corresponding to those years where adequacy risk is highest (cf. Fig. 12). The graph shows how the boom in OCGT investment in expectation of the high gross margins after 2023 is followed by a bust phase around 2026 when large volumes of new nuclear capacity begin entering the system (cf. Fig. 11(b)). This increases the capacity margin but reduces profitability for peaking units. In fact, a significant volume of plant is mothballed toward the end of the simulation time horizon suggesting that generators expect energy market revenues to remain low.

The mothballing of OCGT early in the simulation (2011) is likely to be a direct result of unrealistically high capacity margins out to 2014 (cf. Fig. 10(b)); the existing CCGT builds come online during these years in anticipation of LCPD closures (cf. Section V). To avoid over complicating the plots, the profitability of other technologies is not included, however similar profitability trends were witnessed for CCGT. Investment in OCGT capacity begins around 2014 with similar trends witnessed in CCGT and nuclear, however no coal investments are made (a plot of technology screening curves showed coal as uneconomical relative to the other technologies).

After 2025, very little CCGT or OCGT investment is triggered and endogenous capacity growth is minimal. Nuclear plants experience a sustained period of positive gross margins after 2023, which is attributed to the rising fuel and carbon costs witnessed for fossil-fuel technologies (DECC central case estimates) and hence increasing scarcity rents. Combining this with the data presented in Fig. 11(a), implies a period of intense CCGT and OCGT investment for the 10 years after 2015 to offset retirements to existing capacity and respond to demand growth during 2020-25. Average annual endogenous capacity growth is -2.2% between 2015-25 as a result of 29.7 GW of new thermal build being offset by 42.2 GW of thermal plant retirements (options for lifetime extension not considered here). This suggests that thermal capacity is not replaced on a like-for-like basis, which is hardly surprising given that average growth in installed wind generation is 12% over the same period. The ten years after 2025 provide better growth (average endogenous capacity growth 1.2% between 2026-35), on account of wind capacity levelling off, demand remaining flat and retirements continuing. In fact, nuclear is the only endogenous plant type to increase in terms of total installed capacity for the period 2025-40. This analysis suggests that new investments struggle to recover fixed costs during the period after 2026 owing to growth in nuclear capacity within a high wind system dampening energy market revenues for fossil-fuel generation.

An interesting analysis is to compare simulated real-time (annual) prices with investor expectations. This can be used to determine how well investors predictions of gross margins track those realised. Fig. 14 shows the average simulated competitive prices across the MC runs versus realised competitive prices for 1 and 3 years ahead for each of the years 2010, 2015, 2020 and 2025. Choosing 2020 as an example, in Fig. 14(a) (x-axis), the average of expected simulated competitive price for 2021 (solid line with squares) is higher than the realized price for 2021 (dashed line with triangles) by 12 £/MWh. The degree of difference is also directly related to the volume of plant under construction; the more plant being built, the greater the over-estimation of market prices (and hence gross margins). Furthermore, the proportion of long lead time plant under construction exacerbates this trait. For instance, in 2020 the volumes of OCGT, CCGT and nuclear capacity under construction are 3.9, 5.8 and 3 GW, respectively, where as in 2025 it is 0, 10 and 6.5 GW, respectively, which is the year with the biggest difference. Note that, although mark-ups from market power are not shown here, precisely the same pattern occurs for simulated revenues from mark-ups. This can be traced back to the degree of uncertainty with

which plant under construction is treated by the investor; the exact timings of when new plants will arrive are modelled as stochastic (cf. Section III-A). To test this hypothesis, a sensitivity case was modelled where investors have perfect foresight about investments in the pipeline, this is described in the next section (case 2c).

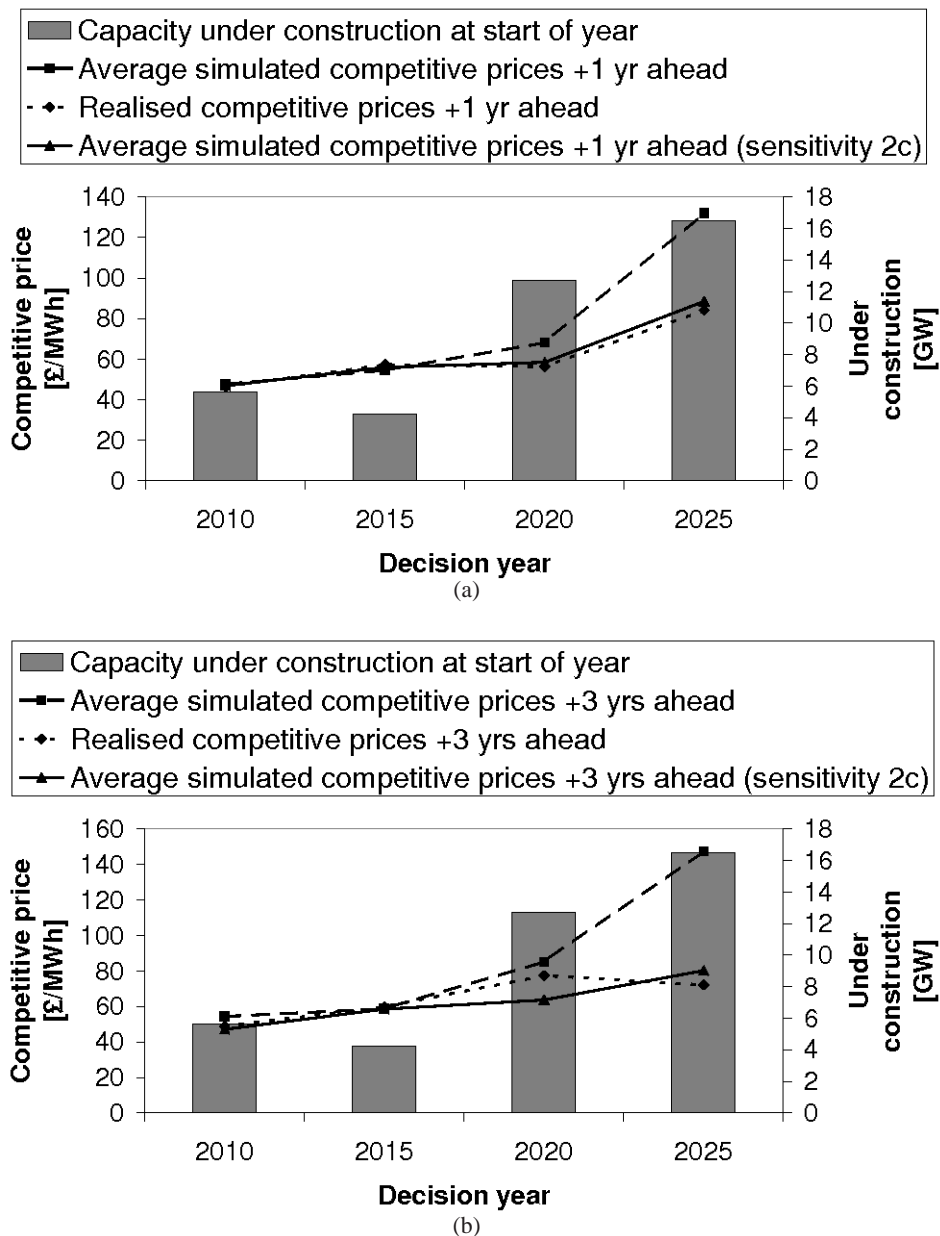


Fig. 14. (a) Plot of expected competitive market prices 1 year ahead from decision year (x-axis) and (b) expected competitive market prices 3 years ahead from decision year. Volume of capacity under construction at time decision is taken also shown in each case (columns).

B. Sensitivity analyses

In order to test the robustness of the model, extensive sensitivity analyses have been performed on a number of model assumptions. Those found to be the most critical, some of which are plotted in Fig. 15 with key associated metrics shown in Tables IV and V, include:

- 1) The level of expected scarcity price (i.e., VOLL). Here, the maximum value of 10,000£/MWh is reduced and the price mark-up function $w(L, G_N^*)$ is altered (cf. Fig. 7(b)) when calculating expected gross margins (37). Experiments using case a) 'VOLL 30000': 30,000 £/MWh and b) 'VOLL 2000': 2,000 £/MWh are carried out.
- 2) Investor expectations about new builds. Taking inspiration from [6], we test case a) the '*believers*' case; here the investor ignores plants under construction when making expectations about revenues. The impact of new builds on prices are only considered once plants are fully operational (i.e., will systematically over-predict market prices). Secondly, case b), the '*pre counter*' is used where the investor views all plant under construction as operational (i.e., will systematically under-predict market prices). Finally, case c), a '*accurate*' investor is modelled where estimates about construction lead times match the delays experienced in reality (i.e., lead times shown in Table III). This last case can be used to test the hypothesis that differences between realised and investor expectations about prices is due to the uncertainty surrounding capacity under construction.
- 3) The aggregate investment response from the market. This is achieved by altering the constant exponent, β , in the aggregate investment response function (9) to a) 0.9, 'Resp. higher' and b) 0.5, 'Resp. lower' (cf. Fig. 2).
- 4) The ability of plant owners to exercise market power and volumes of revenues received by doing so, reference 'No markup'. This is achieved by calculating expected gross margins using (24) instead of (37) (i.e., no price mark-up and a perfectly competitive market).
- 5) Investor risk preferences: achieved by case a) 'VaR higher': increasing critical q to 0.5 in VaR test (cf. Section III-B), case b) 'VaR lower': lowering critical q to 0.01, case c) 'WACC lower': reducing investor WACC and case d) 'WACC higher': increasing investor WACC.
- 6) Increasing investor uncertainty about load growth. Investors still consider load growth to be stochastic, however the standard deviation of the Normal distribution used to sample

load growth is increased from 1% to 3%, reference 'Load SD'.

- 7) Economics of peaking plants: achieved by case a) 'AS reduce': reducing the amount of AS revenue for OCGT plants and case b) 'FC increase': increasing total fixed costs (i.e., $TAFC_x$).

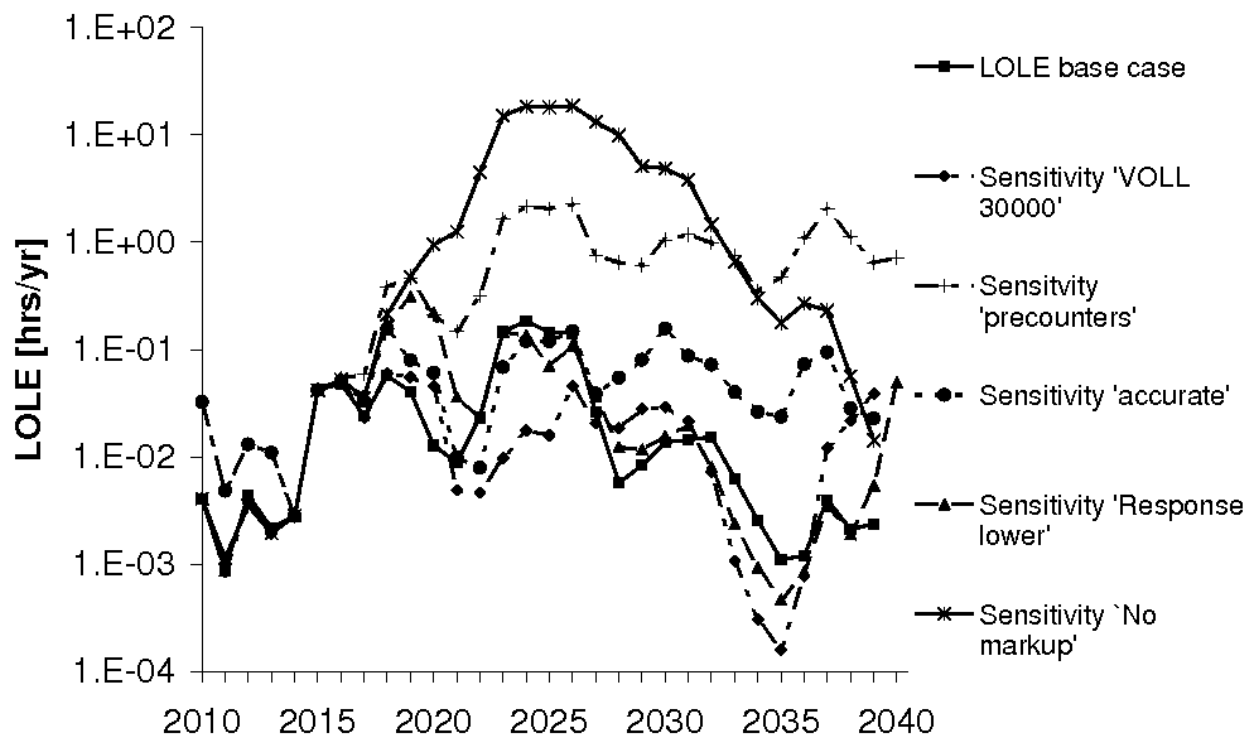


Fig. 15. Plot of simulated LOLE for selected sensitivities (nos. 1-6). Note the logarithmic scale.

Overall, the model's qualitative behaviour was reasonable for the sensitivities listed and provided some useful insights, particularly when comparing the oligopolistic base case to the perfectly competitive market results (i.e., zero price mark-up, see below).

For test case 'VOLL 30000', by increasing the VOLL, the expectation would be to see more investment as price spikes signals are stronger, which could potentially lead to a lower level of risk and also more investment relative to the base case. For test case 'VOLL 2000', by reducing the VOLL, the expectation would be to see delays in investment as price spikes are dampened, which could potentially lead to a higher level of risk and also less investment relative to the base case. For instance, in a perfectly competitive market, in order for an OCGT plant to recover

TABLE IV

FIRST SUMMARY TABLE OF SECURITY OF SUPPLY AND INVESTMENT RESULTS FOR BASE CASE AND SENSITIVITY ANALYSIS. FIGURES IN BRACKETS BELOW EACH CASE FIGURE SHOW STANDARD DEVIATION (SECURITY OF SUPPLY RISK METRICS) OR VOLUME OF PLANT MOTHBALLED (TOTAL INVESTMENT AND MOTHBALLING).

Test	Security of supply risk metrics						Total investment and mothballing			
	Average de-rated margin 2010-40 (%)	Average diff. in margins relative to base case (%)	No. years negative	Deepest shortfall (%yr)	LOLE (hrs/yr)	EEU (GWh)	2010-40 (GW)			
							Nuclear	Coal	CCGT	OCGT
Base case	5.6 (7.1)	-	4	(-6.8, 2024)	0.03 (0.05)	5.7 (9.2)	30.5 -	0 (3.0)	34 (1.2)	12.1 (4.6)
VOLL 30000	6.5 (5.0)	1.2	1	(-1.3, 2025)	0.02 (0.02)	3.3 (3.1)	31.5 -	0 (2.5)	37 (7.8)	15 (10.9)
VOLL 2000	3.8 (7.8)	-3.0	10	(-9.0, 2022)	0.22 (0.49)	46.8 (116.7)	30.5 -	0 (3.0)	32.6 (3.0)	13.3 (5.0)
Believer	12.9 (6.7)	7.0	1	(-2.6, 2018)	0.01 (0.02)	1.9 (4.8)	30.5 0	0 (3.5)	34 0	32.4 (15.0)
Pre counter	-5.1 (8.5)	-10.1	21	(-16.9, 2026)	0.71 (0.70)	158.7 (167.3)	30.5 -	0 (3.0)	27.6 (3.6)	12.0 (5.3)
Accurate	1.7 (4.5)	-3.9	15	(-5.9, 2030)	0.06 (0.05)	10.2 (8.3)	31.0 -	0 (1.5)	24.2 (3.6)	22.9 (6.2)
Resp. higher	6.3 (5.2)	0.8	6	(-4.7, 2024)	0.02 (0.03)	4.0 (5.3)	31.0 -	0 (3.0)	36.8 (5.8)	13.7 (6.6)
Resp. lower	5.0 (5.7)	-0.5	8	(-5.8, 2023)	0.05 (0.08)	8.9 (14.3)	29.0 -	0.5 (2.5)	35.2 (1.0)	19.8 (4.9)
No markup	-8.3 (14.4)	-13.0	20	(-33.2, 2024)	3.9 (6.25)	1474 (2621.2)	31.0 -	0 (1.0)	32.6 (0.6)	8.5 (1.4)

TABLE V
SECOND SUMMARY TABLE OF SECURITY OF SUPPLY AND INVESTMENT RESULTS FOR BASE CASE AND SENSITIVITY ANALYSIS. FIGURES IN BRACKETS BELOW EACH CASE FIGURE SHOW STANDARD DEVIATION (SECURITY OF SUPPLY RISK METRICS) OR VOLUME OF PLANT MOTHBALLED (TOTAL INVESTMENT AND MOTHBALLING).

Test	Security of supply risk metrics						Total investment and mothballing			
	Average de-rated margin 2010-40 (%)	Average diff. in margins relative to base case (%)	No. years negative	Deepest shortfall (% ,yr)	LOLE (hrs/yr)	EEU (GWh)	2010-40 (GW)			
							Nuclear	Coal	CCGT	OCGT
Base case	5.6 (7.1)		4	(-6.8, 2024)	0.03 (0.05)	5.7 (9.2)	30.5 -	0 (3.0)	34 (1.2)	12.1 (4.6)
VaR higher	7.3 (5.2)	1.7	4	(-5.3, 2023)	0.02 (0.03)	3.4 (5.1)	29.5 -	0 (3.5)	30.6 (2.8)	18.2 (6.4)
VaR lower	6.2 (5.0)	0.9	5	(-5.7, 2023)	0.02 (0.03)	4.2 (6.1)	30 -	0 (3.0)	31 (3.6)	16.6 (7.1)
WACC lower	7.0 (4.8)	1.4	4	(-4.9, 2023)	0.02 (0.03)	3.3 (4.8)	30.5 -	0 (3.0)	28.4 (1.0)	7.8 (1.6)
WACC higher	4.8 (4.6)	-0.8	7	(-5.5, 2023)	0.03 (0.04)	5.8 (7.5)	31.5 -	0 (3.0)	39.2 (1.4)	19.1 (4.7)
Load SD	8.5 (5.3)	2.9	3	(-1.9, 2026)	0.01 (0.01)	2.0 (2.4)	30.5 0	0 (2.0)	32.4 (0.8)	22.6 (6.7)
AS reduce	3.9 (5.0)	-1.6	12	(-6.9, 2023)	0.05 (0.07)	9.3 (12.5)	31 -	0 (3.0)	39.2 (5.0)	9.9 (5.1)
FC increase	5.9 (4.3)	0.0	5	(-4.1, 2023)	0.04 (0.04)	7.4 (7.1)	30.5 -	0 (3.0)	38.8 (3.0)	12.8 (14.3)

its fixed costs (47.25 £/unforced kW/yr), the price must reach the VOLL (10,000 £/MWh) in at least 4.7 hrs/yr (actually more to account for short-run MC of production), and reducing the VOLL to 2,000 £/MWh increases this duration to 23.6 hrs/yr. The simulation results showed that increasing the VOLL to 30,000 £/MWh leads to a small improvement in average de-rated margins to 6.5% with a standard deviation of 5.0%. Furthermore, de-rated margins are negative

during only 2026/27. The average annual LOLE reduces to 0.02 hrs/yr with average annual EEU of 3.3 GWh. Interestingly, CCGT investment begins 1 year earlier and has a smoother cumulative profile relative to the base case (standard deviation of year-on-year volumes 0.8 GW versus 1.2 GW in base case). This displaces some OCGT investment early on, but overall volume during 2015-25 increase by 2 GW. Reducing the VOLL to 2,000 £/MWh alters investment timings, but overall volumes are only slightly reduced (3% lower than base case). The average annual LOLE increases to 0.22 hrs/yr with average annual EEU of 46.8 GWh. CCGT investment starts 2 years later relative to the base case, which interestingly increases nuclear investment by 2 GW during 2015-20. OCGT investment is less intense during 2015-18 but volumes are significantly higher during 2020-23 (4.7 GW compared with 1.1 GW). This is in response to higher expected gross margins in 2022-26 as a result of less short lead time plant investment early on.

For test case *'believers'*, the anticipation would be more investment relative to the base case due to the investor now systematically over-estimating revenues because they do not account for the impact of new builds when formulating price expectations. Results produced more investment than under the base case, with more severe over-shoot dynamics witnessed. As a result, average annual LOLE falls to 0.01 hrs/yr with generators unable to recover fixed costs with significant increases in the volume of mothballed OCGT capacity.

For test case *'pre counters'*, the anticipation would be less investment relative to the base case due to the investor now systematically under-estimating revenues because they include new builds before they are operational when formulating their price expectations. Results showed under-investment and average annual LOLE increases to 0.71 hrs/yr. As a result of less investment, overall profitability of existing plant improves, with some mothballing in the early part of the simulation in response to high forecast margins.

For test case *'accurate'*, the expectation would be reduced over-shoot dynamics and better prediction of out-turn prices relative to the base case. This is on account of the investor making a better prediction of the timing of capacity under construction, which is particularly important when there is a lot of long lead time plant (e.g., nuclear) under construction. Simulation results show that nuclear, CCGT and OCGT receive positive gross margins in almost all years after 2015, however average LOLE doubles to 0.06 hrs/yr and with a noticeable oscillation of frequency 5 years and amplitude 0.12 hrs/yr (Fig. 15). Average EEU also increases to 10.2 GWh. Fig. 14 shows a significant improvement in investor price expectations at the 1 year ahead stage,

with expectation 3 years ahead also more akin to reality. Expectations about years 4-7 ahead performed better than the base case, however, due to the possibility of new investments (or mothballing) impacting on those years, significant differences remain.

For test case ‘Resp. lower’, the expectation would be that reductions to the exponent β in (9) to reduce investment, and increases under ‘Resp. higher’ to increase investment. This could also impact on the timing of investments later in the simulation in account of changes to investment levels early on. The results followed expectations; changes produced similar investment timings to the base case for OCGT and CCGT early in the time horizon but the reduced (resp. increased) levels of aggregate response lead to increases (resp. decreases) in generation adequacy risk in the medium-term (out to 2020) but higher (resp. lower) levels of investment later on in response to higher (resp. lower) forecast revenues. In the case of nuclear, a reduced response curve time-slipped the investment pattern by two years from 2020, whereas for the increased response curve the patterns were broadly similar.

For test case ‘No markup’, the perfectly competitive market case, the expectation would be lower overall levels of investment on account of price mark-ups being removed from the revenue calculation. Here more sustained periods of high prices (and hence scarcity rents) are required in order to recover invested capital and receive adequate return on investment. Indeed, when limiting the ability to exercise market power by removal of price mark-up, CCGT investments are most affected. Investment in this technology starts four years later than the base case and cumulative investment is on average 4.4 GW lower. Nuclear investments are also dampened, with investment during the first 15 years of the simulation 3 GW lower than the base case. These dynamics led to an order of magnitude increase in average annual LOLE and EEU to 3.9 hrs/yr and 1474 GWh, respectively. Of course these dynamics may differ in a model representing more sophisticated firms who account for the effect of their investment upon mark-ups for their existing fleet. In this case firms may deliberately not invest in order to keep prices (including mark-ups) high, however this type of investor logic is not considered here.

For test case ‘VaR higher’ and ‘VaR lower’, the expectation would be to see changes to the level of investments, particularly early on when the threshold for investment, which is considered only if the VaR criterion $p(V_x^q > 0) \geq (100 - q)\%$ is met. This means that an investment could be deemed attractive earlier (in the case where $q = 0.5$) or later (in the case where $q = 0.01$) relative to the base case. Moreover, the VaR criterion relates to the degree of risk aversion (cf.

Section III-B), therefore $q = 0.5$ models a less risk averse investor, and $q = 0.01$ models a more risk averse investor. Results of this experiment showed that modelling a less risk averse investor leads to marginally earlier nuclear investment (typically viewed as high risk due to high investment costs and operational inflexibility), with peaking plant investment timings remaining unchanged but volumes increasing in some years. Modelling a more risk averse investor leads to OCGT investment timings remaining unchanged but volumes increasing and displacing some CCGT (5.4 GW overall reduction in CCGT and 3.3 GW increase in OCGT); this is attributed to a higher degree of certainty about prices in the near term, resulting in less variance in projected revenues for short lead time plant. Hence the VaR criterion will tend to favour this type of plant for low values of q .

For test case ‘WACC lower’ and ‘WACC higher’, a similar expectation to that of ‘VaR higher’ and ‘VaR lower’ were held. Results show that the degree of impact that changes to the WACC had on investment timings was related to construction lead time. This is hardly surprising given that investment costs for long lead time plant are highly sensitive to the discount rate used. For instance, increasing required equity by 3% across all technologies delays nuclear investment by 3 years and overall volume by 5.5 GW during 2010-25. This leads to higher generation adequacy risk during 2018-22. Similarly, CCGT investments are delayed by 2 years although volumes are similar in account of the lower nuclear builds increasing expected gross margins and triggering investment. Reducing the equity return by 3% leads to higher and earlier volumes of nuclear investment with annual average LOLE reduced, however gross margins are reduced.

For test case ‘Load SD’, the expectation would be that an increase to the standard deviation of load growth to lead to a higher standard deviation of the distribution of project value. This increased uncertainty surrounding profitability would reduced and/or delay investment. In fact, increasing investor load growth uncertainty leads to less CCGT and nuclear investment out to 2020, however OCGT investment increases by 10 GW over the base case for the period 2019-21 in anticipation of high market prices in 2022-26. This high volume of investment lowers the generation adequacy risk and serves to dampen market prices, and OCGT gross margins are positive in 2026 only (the only year when de-rated margins are negative).

For test case ‘AS reduce’, a reduction in AS revenues (and hence profitability) was expected to reduce OCGT investments, although not massively in account of AS revenues alone not being sufficient to trigger investment (cf. Section III-A). In fact, reducing OCGT AS revenues from

10,000/MW/yr to 5,000/MW/yr alters investment timings and capacity choice early on in the simulation, however long-term overall volumes are only marginally affected. More precisely, a reduction in OCGT investment during 2014-2018 (1.6 GW compared with 11 GW in base case) is somewhat offset by increases in CCGT (8.8 GW compared with 4.6 in base case) and nuclear (up 2.5 GW on base case) investment during this period. All three technologies were deemed profitable during this period; the model chooses the technology with the highest PI (10) and iterates until no additional plants are profitable (cf. Section III-C). A reduction in AS revenues for OCGT means that other technologies have more favourable profitability in the first iteration of the investment decision. OCGT is not chosen in subsequent iterations as a result of other capacity additions reducing its profitability to suboptimal levels. By choosing to invest in longer lead time plant, total LOLE over 2019-2023 increases from 0.29 to 0.97 hrs. Interestingly, higher volumes of OCGT investment occur in these later years (5.6 GW during 2019-2020 compared with 1.1 GW in base case). This is likely to be a consequence of the increased volumes of longer lead time plant under construction during this period increasing the differences between investor price predictions and reality (i.e., as discussed in sensitivity 2c).

Finally, for case 'FC increase', increasing OCGT $T AFC_x$ from 42.5 to 60 £/MW/yr was expected to produce similar dynamics to 'AS reduce'. This turned out to be the case, however the increase in LOLE is less severe (although still higher than the base case).

In summary, a pattern of increased relative levels of risk and erosion of de-rated capacity margins was experienced during the 2020s to some degree in all cases. Furthermore, the period of highest security of supply risk is 2023-28, however the magnitude of the risk (measured by LOLE) differs between experiments. A prolonged period of increased security of supply risk is experienced throughout the 2020s for the perfectly competitive market case. Also, providing investors with perfect foresight about capacity under construction produces less investment and more frequent periods of relatively high LOLE and low de-rated margins after 2020. However, generators experience positive gross margins in more years on account of reduced surplus margins, and hence higher prices.

The 2020s is the period of most intense change; during this decade over 40 GW of new capacity is built with over 34 GW retiring; 14.5 GW of capacity leaves the system during the period 2023-26 alone. This further exacerbates the higher relative levels of risk during this period. Furthermore, no new coal investments are made, with the majority of new investment coming

from gas-fired generation. That said, however, a sensitivity on the primary fuel prices is not included here. For instance, lower coal prices (or indeed higher gas prices) may lead to different technology choice, however the impact on overall volumes (and hence relative levels of risk) is likely to remain unchanged.

VII. CONCLUSION

The MOND technique to calculate expected output, costs and revenues of thermal generation subject to varying load and random independent thermal outages has been presented. This method has been adapted for use in a dynamic capacity market model with high penetrations of wind by performing a residual load calculation with simulated wind outputs. An ‘energy-only’ market setting has been used to estimate the economic profitability of capacity investments. Using relative levels of de-rated capacity margin and LOLE as the risk metric, simulation results for GB show that levels of generation investment lead to a mild increase in generation adequacy risk in some years, with erosion of de-rated capacity margins in the mid 2020s, and very tight supply conditions are experienced during a small number of peak hours. Many new investments, particularly peaking units, were unable to recover their fixed costs. A sensitivity analysis demonstrated that assumptions about investor risk profiles and expectations about new builds, load growth and the ability to exercise market power have a strong impact on simulated investment dynamics and subsequent levels of generation adequacy risk. However a relative increase in generation adequacy risk in the mid 2020s was experienced across all experiments, with increases occurring earlier and more severely in some cases.

A key goal for policy makers is to ensure that liberalised energy markets incentivise timely and sufficient thermal generating capacity investment in order to compliment increasing penetrations of variable output generation such as wind. This is particularly true of peaking generation and energy storage technologies. Due to their low utilisation factors, these units will rely on being dispatched at high prices in order to recover their fixed costs and provide adequate returns on investment. Results presented here suggest that revenues from an ‘energy-only’ market are insufficient and additional mechanisms may be required. Moreover a sensitivity analyses demonstrated that investor expectations about wholesale prices, in particular the demand-side’s willingness to pay and the damping effect that new builds have on revenues, exacerbate the risk of investment shortfalls. This has significant policy implications for GB where sizeable demand

response and new smart-loads are expected to emerge. Whether or not these entities will in fact respond to high wholesale prices by reducing consumption remains to be seen. However if generators anticipate a price responsive demand-side and it fails to emerge, then a relative increase in the risk of investment shortfall is likely to occur.

The topic of subsequent research will be to determine whether explicit capacity mechanisms such as tendering for strategic reserve (e.g., [40]) and capacity markets (e.g., [14]) can be designed to alleviate resource shortfall and prevent investment overshoot. The results here indicate that such a mechanism may be desirable to improve reserve margins in the mid 2020s in GB.

ACKNOWLEDGMENT

The authors acknowledge valuable input from C. Dent, S. Hawkins, T. Johnson and G. P. Harrison. Also thanks to EPRG, in particular D. Newbery, for facilitating this collaboration. This research formed part of the UKERC programme and was supported by the UK Research Councils under NERC award NE/C513169/1. Partial support for B.F. Hobbs was provided by the U.K. EPSRC Supergen Flexnet program and the U.S. National Science Foundation through EFRI Grant 0835879.

REFERENCES

- [1] H. Balériaux, E. Jamouille, and F. Linard de Guertechin, "Simulation de L'Exploitation d'un Parc de Machines Thermiques de Production D'Électricité Couplé à des Stations de Pompage," *Revue E de la Société Royale Belge des Electriciens*, vol. 7, pp. 225–245, 1967.
- [2] R. Booth, "Power System Simulation Model Based on Probability Analysis," *IEEE Trans. Power Apparatus and Systems*, vol. PAS-91, no. 1, pp. 62–69, Jan. 1972.
- [3] G. Gross, N. Garapic, and B. McNutt, "The Mixture of Normals Approximation Technique for Equivalent Load Duration Curves," *IEEE Trans. Power Systems*, vol. 3, no. 2, pp. 368–374, May 1988.
- [4] J. G. Iñón, "Long-run Probabilistic Production Costing-Based Analysis of Electricity Market Designs for Long-Run Generation Investment Incentives under Spot-Pricing and Transmission Open-Access," Ph.D. dissertation, John Hopkins University, 2011, in preparation.
- [5] B. F. Hobbs, J. Iñón, and S. E. Stoft, "Installed Capacity Requirements and Price Caps: Oil on the Water, or Fuel on the Fire?" *The Electricity Journal*, vol. 14, no. 6, pp. 23 – 34, 2001.
- [6] A. Ford, "Waiting for the Boom: a Simulation Study of Power Plant Construction in California," *Energy Policy*, vol. 29, no. 11, pp. 847 – 869, 2001.
- [7] S. Gary and E. R. Larsen, "Improving Firm Performance in Out-of-Equilibrium, Deregulated Markets Using Feedback Simulation Models," *Energy Policy*, vol. 28, pp. 845–855, 2000.

- [8] F. Olsina, F. Garces, and H.-J. Haubrich, "Modeling Long-Term Dynamics of Electricity Markets," *Energy Policy*, pp. 1411–1433, 2006.
- [9] T. Kayoda, S. Ihara, E. Larose, M. Sanford, A. K. Graham, C. A. Stephens, and C. K. Eubanks, "Utilizing System Dynamics Modeling to Examine Impact of Deregulation on Generation Capacity Growth," in *Proceedings of the IEEE*, vol. 93, no. 11, Nov 2005.
- [10] B. Hobbs and Y. Ji, "A Bounding Approach to Multiarea Probabilistic Production Costing," *IEEE Trans. Power Systems*, vol. 10, no. 2, pp. 853–859, May 1995.
- [11] A. Bar-Ilan, A. Sulem, and A. Zanello, "Time-to-build and Capacity Choice," *Journal of Economic Dynamics and Control*, vol. 26, no. 1, pp. 69–98, January 2002.
- [12] E. R. Larsen and D. W. Bunn, "Deregulation in Electricity: Understanding Strategic and Regulatory Risk," *The Journal of the Operational Research Society*, vol. 50, no. 4, pp. 337–344, April 1999.
- [13] J. F. Muth, "Rational Expectations and the Theory of Price Movements," *Econometrica*, vol. 29, no. 3, pp. 315–335, July 1961.
- [14] B. F. Hobbs, M.-C. Hu, J. G. Iñón, S. E. Stoft, and M. P. Bhavaraju, "A Dynamic Analysis of a Demand Curve-Based Capacity Market Proposal: The PJM Reliability Pricing Model," *IEEE Trans. Power Systems*, vol. 22, no. 1, pp. 3–14, Feb. 2007.
- [15] Department of Energy and Climate Change, "Communication on DECC Fossil Fuel Price Assumptions," www.decc.gov.uk/en/content/cms/about/ec_social_res/analytic_projs/ff_prices/ff_prices.aspx.
- [16] —, "First Annual Update of the Short Term Traded Carbon Values (June 2010)," www.decc.gov.uk/en/content/cms/what_we_do/lc_uk/valuation/valuation.aspx.
- [17] ICE Futures Europe, "Report Center; End of Day Reports (UK Natural Gas & Newcastle Coal Futures)," www.theice.com/marketdata/reports/ReportCenter.shtml.
- [18] A. Cartea and M. Figueroa, "Pricing in Electricity Markets: a Mean Reverting Jump Diffusion Model with Seasonality," *EconWPA, Finance 0501011*, Jan. 2005.
- [19] A. Dixit and R. Pindyck, *Investment Under Uncertainty*. Princeton University Press, 1994.
- [20] "Our Electricity Transmission Network: A Vision for 2020," ENSG, Tech. Rep., www.ensg.gov.uk/index.php?article=126.
- [21] World Nuclear Association, "The Economics of Nuclear Power," www.world-nuclear.org/info/inf02.html.
- [22] "UK Electricity Generation Costs Update," Mott MacDonald, Tech. Rep., June 2010, www.decc.gov.uk/en/content/cms/about/ec_social_res/analytic_projs/gen_costs/gen_costs.aspx.
- [23] P. Artzner, F. Delbaen, J.-M. Eber, and D. Heath, "Coherent Measures of Risk," *Mathematical Finance*, vol. 9, no. 3, pp. 203–228, 1999.
- [24] D. Eager, J. W. Bialek, and T. Johnson, "Validation of a Dynamic Control Model to Simulate Investment Cycles in Electricity Generating Capacity," in *Power and Energy Society General Meeting, 2010 IEEE*, July 2010, pp. 1–8.

- [25] R. Billinton and R. N. Allan, *Reliability Evaluation of Power Systems. 2nd ed.* Plenum, 1994.
- [26] J. Endrenyi, *Reliability Modeling in Electric Power Systems.* Wiley, 1978.
- [27] S. Stoft, *Power System Economics Designing Market for Electricity.* IEEE Press: Wiley, 2002, pp. 70–71.
- [28] J. Boucher and Y. Smeers, “Alternative Models of Restructured Electricity Systems, Part 1: No Market Power,” *Operational Research*, vol. 49, pp. 821–838, Nov. 2001.
- [29] C. Metzler, B. F. Hobbs, and J.-S. Pang, “Nash-Cournot Equilibria in Power Markets on a Linearized DC Network with Arbitrage: Formulations and Properties,” *Networks and Spatial Economics*, vol. 3, pp. 123–150, 2003.
- [30] Pöyry, “Impact of Intermittency: How Wind Variability Could Change the Shape of the British and Irish Electricity Markets,” July 2009, www.poyry.com/linked/group/study.
- [31] R. Sioshansi and S. Oren, “How Good are Supply Function Equilibrium Models: an Empirical Analysis of the ERCOT Balancing Market,” *Journal of Regulatory Economics*, vol. 31, pp. 1–35, 2007.
- [32] J. B. Bushnell, E. T. Mansur, and C. Saravia, “Vertical Arrangements, Market Structure, and Competition: An Analysis of Restructured US Electricity Markets,” *American Economic Review*, vol. 98, no. 1, pp. 237–66, 2008.
- [33] P. Visudhiphan, “Dynamic Investment in Electricity Markets and Its Impact on System Reliability,” in *Market Design 2001 Conference, Stockholm*, 2001, pp. 91–110.
- [34] J. Valenzuela and M. Mazumdar, “Cournot Prices Considering Generator Availability and Demand Uncertainty,” *IEEE Trans. Power Systems*, vol. 22, no. 1, pp. 116–125, Feb. 2007.
- [35] P. E. O. Aguirre, C. J. Dent, G. P. Harrison, and J. W. Bialek, “Realistic Calculation of Wind Generation Capacity Credits,” in *Integration of Wide-Scale Renewable Resources Into the Power Delivery System, 2009 CIGRE/IEEE PES Joint Symposium*, July 2009, pp. 1–8.
- [36] Personal communication S. Hawkins and G. P. Harrison, Institute for Energy Systems, University of Edinburgh.
- [37] Met Office Unified Model, www.metoffice.gov.uk/science/creating/daysahead/nwp/um.html.
- [38] S. Hawkins, D. Eager, and G. P. Harrison, “Characterising the Reliability of Production from Future British Offshore Wind Fleets,” in *Renewable Power Generation Conference, 2011. IET*, to be published in 2011.
- [39] RenewableUK, www.bwea.com/offshore/index.html.
- [40] Department of Energy and Climate Change, “Electricity Market Reform Consultation Document,” Tech. Rep., December 2010, www.decc.gov.uk/en/content/cms/consultations/emr/emr.aspx.
- [41] “Seven Year Statements,” National Grid, Tech. Rep., www.nationalgrid.com/uk/Electricity/SYS/.
- [42] “Winter Outlook Consultation 2010/11,” National Grid, Tech. Rep., www.nationalgrid.com/uk/Gas/TYS/outlook/.
- [43] Department of Energy and Climate Change, “Energy and Emissions Projections,” www.decc.gov.uk/en/content/cms/about/ec_social_res/analytic_projs/en_emis_projs/en_emis_projs.aspx.
- [44] S. Zachary, C. Dent, and D. Brayshaw, “Challenges in Quantifying Wind Generation’s Contribution to Securing

Peak Demand,” in *Power and Energy Society General Meeting, 2011 IEEE*, July 2011, pp. 1 –8.

[45] Economic and Social Data Service, www.esds.ac.uk/international/access/dataset_overview.asp#desc_ieaei.

[46] Digest of United Kingdom Energy Statistics, “Chapter 5: Electricity, Tables 5.6 and 5.7,” www.decc.gov.uk/en/content/cms/statistics/publications/dukes/dukes.aspx.

Dan Eager received the B.Sc. degree in mathematics and computer science from The University of Sussex in 2004, and the M.Sc. degree in operational research from The University of Edinburgh in 2007. He is currently undertaking a Ph.D. within The University of Edinburgh’s Institute for Energy Systems under the supervision of G. Harrison, J. Bialek and T. Johnson.

Benjamin F. Hobbs received the Ph.D. degree in environmental system engineering from Cornell University, Ithaca, NY, in 1983. He is Schad Professor of Environmental Management at the Johns Hopkins University, Baltimore, MD. In 2009-2010 he was on sabbatical at the Electricity Policy Research Group at the University of Cambridge. He chairs the California ISO Market Surveillance Committee and is Director of the JHU Environment, Energy, Sustainability & Health Institute.

Janusz W. Bialek is Professor of Electrical Power and Control with the School of Engineering and Computing Sciences, Durham University, UK. He holds M.Eng (1977) and Ph.D. (1981) degrees from Warsaw University of Technology, Poland. In 1981-1989 he was with Warsaw University of Technology, in 1989-2002 with Durham University, UK, and in 2003-2009 with The University of Edinburgh. He has co-authored 2 books and over 100 technical papers.

APPENDIX A
ABBREVIATIONS & FORMULA VARIABLES

A. Abbreviations

AS	-	Ancillary services
BM	-	Balancing market
CCGT	-	Combined cycle gas turbine
cdf	-	Cumulative distribution function
DDE	-	Delay Differential Equation
DECC	-	Department of Energy and Climate Change
DC	-	De-rated capacity
ELDC	-	Effective load duration curve
EEU	-	Expected energy unserved
FOR	-	Forced outage rate
GQ	-	Gaussian quadrature
GB	-	Great Britain
LCPD	-	Large Combustion Plant Directive
LDC	-	Load duration curve
LOLE	-	Loss-of-load Expectation
MOND	-	Mix of Normals distribution
MC	-	Monte Carlo
NPV	-	Net Present Value
PL	-	Most probable peak load
PJM	-	Pennsylvania-New Jersey-Maryland
PI	-	Profitability Index
OCGT	-	Open cycle gas turbine
r.v.	-	Random variable
SO	-	System Operator
WACC	-	Weighted average cost of capital
VaR	-	Value at Risk
VOLL	-	Value of Lost Load

B. Formula variables

α_x	- Operating lifetime (technology type x)
α	- Speed of mean reversion
β	- Calibrated exponential constant in aggregate investment response function
χ	- Gearing ratio
$\delta(t)$	- Dirac delta function
ϵ	- Required equity investor return
γ	- Expected bond return
η_x	- Time investment capacity block triggered (technology type x)
μ	- Mean of distribution
π_i	- Wholesale price when generator i is at the margin
ρ	- Forced outage rate
σ	- Standard deviation of distribution
τ_x	- Build time (technology type x)
ξ_x	- Investment capacity block (technology type x)
ξ_{max}	- Maximum annual investment per technology
ψ_x	- Vector of new build capacity blocks (technology type x)
Φ	- cdf of Normal distribution
a	- Scalar in wholesale price mark-up function
b	- Exponent in wholesale price mark-up function
c	- Capacity
e_n	- Expected energy served by generator type n
$f(M)$	- pdf of the surplus margin M_N
$f(M_{N-1}, M_N)$	- Joint distribution of capacity margins M_{N-1} and M_N
h_n	- Probability generator n is on the margin
i_x	- Constant used to calibrate aggregate investment response function (technology x)
$mc(L, G_1, G_2, \dots, G_N)$	- Marginal production cost of meeting the load L
m_u	- Number of units of type n
$m(t)$	- Stochastic process time dependent mean reverting level at time t
p_x	- Construction cost (technology type x)
p_n^{disp}	- Probability that a MW belonging to generator n is dispatched
$q(t)$	- DECC fuel price estimate at time t
r	- Weighted Average Cost of Capital
v	- Integral upper bound in (30), (31), (32), and (31) above which price mark-up is negligible owing to the large surplus margin

$w(L, G_N^*)$	- Wholesale price mark-up function
A_x^{crf}	- Deferred CRF (technology type x)
AGM_x	- Gross margins over fixed operating costs (technology type x)
$C_n(P)$	- Total variable operating cost of generator type n , power output P
CGM_n	- Expected annual perfectly competitive gross margin
DC_x	- Present worth of the decommissioning cost (technology type x)
$E(G_n)$	- Expected available capacity from generator type n
FC_x	- Fixed costs (technology type x)
F_t	- Fuel cost at time t
G	- Generator expected available capacity
G_N^*	- Total available generation
$G_N^* - L$	- Overall capacity margin
GM_x^i	- Expected annual gross margin (technology type x , year i)
GM_n	- Expected annual gross margin for generator n
IC_x	- Present worth of investment cost (technology type x)
I_x	- Installed capacity (technology type x)
$I(t)$	- Total installed capacity at time t
$L_{n-1}(x)$	- Load still to be met after adding generator type $n - 1$
$L_n(x)$	- Load still to be met after adding generator type n
$L_{N+1}(0)$	- Probability that there will be insufficient generation to meet demand
MC_i	- Marginal cost of generator i
M_i^x	- Capital expenditure vector (technology type x , year i)
M_{n-1}	- Surplus margin after L has been met using all available generation lower in the merit order than n
N	- Total number of psuedo-generators
PI_x^q	- Profitability index (technology type x)
R_n^i	- Expected gross margin for a particular MW of capacity belonging to generator n when generator i is at the margin
R_n^{L, G_N^*}	- Gross margin received by a MW of capacity from generator n for load L and total available generation G_N^*
RPM_n	- Expected revenue from price mark-up
$T AFC_x$	- Total annualised costs per unforced MW
$TIAC_x$	- Total interest accumulated during construction
V_x	- NPV of an investment (for technology x)
V_x^{opt}	- Minimal acceptable V_x (for technology x)
W	- Standard one-dimensional Brownian motion